THS



LIBRARY Michig. State University

This is to certify that the thesis entitled

EFFECT OF SCALE DURING ELECTROCHEMICAL DEGRADATION OF NAPHTHALENE AND SALICYLIC ACID

presented by

DONG GEUN LEE

has been accepted towards fulfillment of the requirements for the

M.S.	degree in	Civil Engineering
	1000	
		luc
	Major Pro	fessor's Signature
	22/	Aug 2008
		0
		Date

MSU is an affirmative-action, equal-opportunity employer

PLACE IN RETURN BOX to remove this checkout from your record.

TO AVOID FINES return on or before date due.

MAY BE RECALLED with earlier due date if requested.

DATE DUE	DATE DUE
	DATE DUE

5/08 K:/Proj/Acc&Pres/CIRC/DateDue.indd

EFFECT OF SCALE DURING ELECTROCHEMICAL DEGRADATION OF NAPHTHALENE AND SALICYLIC ACID

Ву

Dong Geun Lee

A THESIS

Submitted to
Michigan State University
in partial fulfillment of the requirements
for the degree of

MASTER OF SCIENCE

Civil Engineering

2008

ABSTRACT

EFFECT OF SCALE DURING ELECTROCHEMICAL DEGRADATION OF NAPHTHALENE AND SALICYLIC ACID

By

Dong Geun Lee

Polycyclic aromatic hydrocarbons (PAHs) are a class of organic compounds that consists of two or more benzene rings and they are highly recalcitrant molecules due to their hydrophobicity and low solubility in water. At the laboratory scale, electrochemical degradation of naphthalene and salicylic acid was investigated to evaluate the effect of size of electrochemical cell (1 L versus 3.5 L), AC versus DC current, current density (1 mA/cm² and 3 mA/cm²), and aqueous versus sandy soil media. The tests were carried out in undivided cells immersed in water baths to control the temperature rise.

The key results of this study are: (1) for a given current density, the rate of degradation of naphthalene or salicylic acid was independent of the size of the cell; (2) the energy consumption per unit volume of the electrolyte was 2 to 4 fold greater for the larger cell; (3) while rate of degradation was greater for DC compared to AC for equal current densities, the increase in the rate of degradation was much higher for AC than DC when the electrolyte was continuously stirred; and (4) organic acids can find soil particles containing oxides near the cathode region as ideal sites for adsorption where the degradation is slower when DC is used. However, AC will not allow such adsorption and may be more effective in degradation across the entire sample volume.

ACKNOWLEDGEMENT

This project has been partially funded by 2007 I/UCRC-MTP fellowship and Grant No. BES-0402772 from the National Science Foundation (NSF). This thesis has not been reviewed by the NSF.

I would like to thank all those individuals who helped me in with the research experiments related to my masters thesis. I am grateful to my major advisor Dr. Milind V. Khire who helped me whenever I was in need. I am also thankful to my committee members Dr. Irene Xagoraraki and Dr. Hui Li for their valuable time and support. I also acknowledge the help extended by my lab mates Dr. Emmanuel Pepprah, Moumita Mukherjee, Ramil Mijares, and Carolyn Hardt during the research experiments.

I would like to thank my wife Mrs. Misuk Lee who has been my side to support me. I am also thankful to my parents and parents-in-law for their sincere love and belief in me. Finally, I would like to thank my friends back in the Republic of Korea and here in the U.S. for their constant encouragement and support.

I express my gratitude to Republic of Korea Army for giving me an opportunity and financial support to obtain Masters Degree at Michigan State University. Specially, I would like to thank to LTC, Yongjae Lee, and Moonkyoung Kim for their encouragement.

TABLE OF CONTENTS

LIST OF TABLES	vii
LIST OF FIGURES	viii
CHAPTER 1: INTRODUCTION	1
1.1 OCCURRENCE OF PAHs IN WATER	1
1.2 EXISTING REMEDIATION TECHNIQUES 1.2.1 Advanced Oxidation Processes (AOPs) 1.2.2 Permeable Reactive Barriers (PRBs) 1.2.3 Membrane Processes 1.2.4 Electrokinetic Remediation 1.2.5 Granular Activated Carbon (GAC) Adsorption	2 2 3
1.3 OBJECTIVES 1.3.1 Key Challenges 1.3.2 Target Contaminants 1.3.3 Key Objectives	3 4 5
CHAPTER 2: ELECTOCHEMICAL DEGRADATION	7
2.1 DEGRADATION MECHANISM 2.1.1 Direct Electrolysis 2.1.2 Indirect Electrolysis	7
2.2 FACTORS AFFECTING ELECTROCHEMICAL DEGRADATION 2.2.1 Electrodes 2.2.2 Supporting Electrolyte 2.2.2.1 Sodium Chloride (NaCl) 2.2.2.2 Sodium Sulfate (Na ₂ SO ₄) 2.2.3 Current Type 2.2.4 Current Density	9 10 10 11
2.3 INDEX OF EFFICIENCY 2.3.1 Instantaneous Current Efficiency (ICE). 2.3.2 Electric Energy. 2.3.3 Pollutant Breakdown Rate per Charge. 2.3.4 Electrical Efficiency (Long Order Reduction).	12 13
2.4 MASS TRANSFER REACTION: THE NERNST-PLANCK EQUATION	14

CHAPTER 3: EXPERIMENTAL METHODOLOGY	16
3.1 EXPERIMENTAL SETUP	17
3.1.1 Reaction Chamber	
3.1.1.1 Titanium Electrode	
3.1.1.2 Cell Volume (1 L Cell vs. 3.5 L Cell)	
3.1.2 Electrical Equipment	
3.1.3 Spiked Medium Preparations	
3.1.3.1 Naphthalene in Aqueous Solution	
3.1.3.2 Salicylic Acid in Aqueous Solution	
3.1.3.3 Sand Spiked with Naphthalene or Salicylic Acid	
3.1.4 Stirring Apparatus	
3.2 TESTING, SAMPLING AND ANALYZING TECHNIQUES	29
3.2.1 Sampling Technique	
3.2.1.1 Sampling Frequency	
3.2.1.2 Sampling Method	
3.2.2 HPLC Analysis	
3.2.3 Duplicate Sampling.	
3.2.3 Duplicate Sampling	32
3.3 MONITORED EXPERIMENTAL PARAMETERS	33
3.4 RECYCLING SOILS AND ELECTRODES	35
3.4.1 Soil Recycling	35
3.4.2 Electrode Recycling	37
CHAPTER 4: RESULT AND DISCUSSION	38
4.1 AQUEOUS PHASE EXPERIMENTS	38
4.1.1 Naphthalene	
4.1.1.1 Effect of Current Density on Naphthalene Degradation	
4.1.1.2 Effect of Current Type (AC vs. DC) on Naphthalene Degrad	
4.1.1.3 Effect of Size of Reaction Cells on Naphthalene Degradation	
4.1.1.4 Degradation Kinetics	
4.1.1.5 Cumulative Electrical Energy Consumption	
4.1.1.6 Measured Initial and Final Test Parameters	
4.1.2 Salicylic Acid	
4.1.2.1 Effect of Current Density on Salicylic Acid Degradation n	
4.1.2.2 Effect of Current Type (AC vs. DC) on Salicylic Acid Degra	
4.1.2.3 Effect of Scale of Cells on Salicylic Acid Degradation	
4.1.2.4 Degradation Kinetics	
4.1.2.5 Cumulative Electrical Energy Consumption	
4.1.3 Effect of Stirring During Electrochemical Degradation of Salicylic	
4.1.3.1 Degradation Kinetics	
4.1.3.2 Effect of Stirring on Degradation Rate of Salicylic Acid	
4.1.3.3 Cumulative Energy Consumption	58

4.1.3.4 Measured Initial and Final Test Parameters	59
4.2 SANDY SOIL PHASE EXPERIMENTS	61
4.2.1 Naphthalene	61
4.2.1.1 Rate of Degradation	
4.2.1.1 Cumulative Electrical Energy Consumption	
4.2.2 Salicylic Acid	
4.3 ANALYTICAL MODELING USING NERNST-PLANCK EQUATION	71
4.3.1 Key Assumptions	71
4.3.2 Naphthalene	
4.3.3 Salicylic Acid	74
CHAPTER 5: SUMMARY AND CONCLUSIONS	76
REFERENCES	78

LIST OF TABLES

Table 1.1: Properties of naphthalene and salicylic acid
Table 3.1: Dimensions of electrodes, glass beaker, and Teflon cap22
Table 3.2: Physical properties of 1 L and 3.5 L cells
Table 3.3: Currents densities and equivalent currents for 1 L to 3.5 L cells24
Table 3.4: Preparation of standard solutions for naphthalene and salicylic acid32
Table 4.1: Summary of aqueous phase experiments
Table 4.2: Degradation rate constant (k) and the corresponding half-life $(t_{1/2})$ for naphthalene tests in aqueous solution (time period = 24 hours)43
Table 4.3: Comparison of electrical energy consumption costs for 1 L and 3.5 L cells45
Table 4.4: Summary of key physical parameters for naphthalene tests in aqueous solution
Table 4.5: Degradation rate constant (k) and the corresponding half-life $(t_{1/2})$ for salicylic acid tests in aqueous solution (time period = 24 hours)
Table 4.6: Degradation rate constant (k) and the corresponding half-life $(t_{1/2})$ for salicylic acid tests in stirring aqueous solution (time period = 24 hours)55
Table 4.7: Summary of key parameters for salicylic acid tests in aqueous solution measured at initial and final time elapsed
Table 4.8: Summary of experimental variables for sandy soil phase experiments61
Table 4.9: Summary of key parameters for salicylic acid tests in sandy soil measured at initial and final time elapsed

LIST OF FIGURES

Figure 2.1: Scheme of pollutant removal pathways in electrochemical oxidation7
Figure 3.1: Schematic of testing procedures
Figure 3.2: Representation of experimental setup
Figure 3.3: Picture of a reaction chamber for the 3.5 L cell
Figure 3.4: Schematic of the titanium electrodes, assembled cell, and Teflon cap21
Figure 3.5: Pictures of cap attached to electrodes (top) and the two cells having 1 L and 3.5 L volume (bottom)
Figure 3.6: Pictures of electrical equipment used in the setup: power supply (top), function generator (middle), and digital oscilloscope (bottom)25
Figure 3.7: Pictures of materials used in spiked medium preparations27
Figure 3.8: Pictures of stirrer with 3.5 L cell (top), stirrer (bottom, left), and magnetic bars (bottom, right)
Figure 3.9: Pictures of syringes equipped with needles of different lengths (top) and amber vials with caps used for HPLC analyses (bottom)30
Figure 3.10: Pictures of HPLC instrument
Figure 3.11: Pictures of measuring devices
Figure 3.12: Pictures of procedure followed for cleaning and recycling used sand36
Figure 3.13: Picture while polishing an electrode to clean the fouled electrode surface37
Figure 4.1: Normalized concentration of naphthalene in aqueous phase experiments for DC (a); and AC ($f = 0.1$ Hz) (b) performed at j_{eqv} of 1 and 3 mA/cm ² in 1 L and 3.5 L cells
Figure 4.2: Degradation rate constant (k) and the corresponding half-life $(t_{1/2})$ for naphthalene tests in aqueous solution (time period = 24 hours)43
Figure 4.3: Cumulative normalized electric energy consumed during electrochemical degradation of naphthalene in aqueous phase experiments for DC and AC ($f = 0.1 \text{ Hz}$) performed at j_{eqv} of 1 mA/cm ² in 1 L and 3.5 L cells

Figure 4.4: Normalized concentration of salicylic acid in aqueous phase experiments for DC (a) and AC ($f = 0.1 \text{ Hz}$) (b) performed at j_{eqv} of 1 and 3 mA/cm ² in the 1 L and 3.5 L cells
Figure 4.5: Variation of k observed for salicylic acid tests in aqueous solution52
Figure 4.6: Normalized cumulative electrical energy consumed during electrochemical degradation of salicylic acid in aqueous phase experiments for j_{eqv} of 1 and 3 mA/cm ² in 1 L and 3.5 L cells
Figure 4.7: Variations of k observed for salicylic acid tests in aqueous solution with stirred or without stirred
Figure 4.8: Normalized concentration of salicylic acid in aqueous phase experiments for DC (a) and AC ($f = 0.1$ Hz) (b) performed at $j_{eqv} = 3$ mA/cm ² in 1 L and 3.5 L cells when stirred or unstirred
Figure 4.9: Cumulative electrical energy consumed during electrochemical degradation of salicylic acid in aqueous phase experiments for DC and AC ($f = 0.1$ Hz) performed at $j_{eqv} = 3$ mA/cm ² in 1 L and 3.5 L cells when stirred or unstirred
Figure 4.10: Normalized concentration of naphthalene for aqueous phase and sandy soil phase experiments for DC performed at $j_{eqv} = 1 \text{ mA/cm}^2$ (212 mA) for 3.5 L cell62
Figure 4.11: Cumulative normalized electrical energy consumed during degradation of naphthalene for aqueous phase and sandy soil phase experiments with DC performed at $j_{eqv} = 1 \text{ mA/cm}^2$ for 3.5 L cell
Figure 4.12: Normalized concentration of salicylic acid for aqueous phase and sandy soil phase experiments for DC performed at $j_{eqv} = 1 \text{ mA/cm}^2$ for 1 L and 3.5 L cells64
Figure 4.13: Cumulative normalized electrical energy consumed during electrochemical degradation of salicylic acid in aqueous phase and sandy soil phase experiments for DC performed at j_{eqv} of 1 mA/cm ² in 1 L and 3.5 L cells
Figure 4.14: Normalized concentration of salicylic acid in sandy soil phase experiments for DC (a) and AC ($f = 0.1$ Hz) (b) performed at $j_{eqv} = 1$ mA/cm ² in 1 L and 3.5 L cells67
Figure 4.15: Normalized concentration of salicylic acid across the cell in sandy soil phase experiments for DC performed at $j_{eqv} = 1 \text{ mA/cm}^2$ (212 mA) for 3.5 L cell
Figure 4.16: Experimental and predicted concentration rations of naphthalene for $j_{eqv} = 1$ and 3 mA/cm ² in 1 L and 3.5 L cells for DC application

gure 4.17: Experimenta	l and predicted concentration ratio	os of salicylic acid for $j_{eqv} = 1$
A/cm^2 (a) and 3 mA/cm	2 (b) in 1 L and 3.5 L cells	75

•

LIST OF ABBREVIATIONS

AC = Alternating Current

ATSDR = Agency for Toxic Substance and Disease Registry

AV = Alternating Voltage

DC = Direct Current

DI = De-ionized

DO = Dissolved Oxygen

EIA = Energy Information Administration

HPLC = High Performance Liquid Chromatography

LCR = Inductance, Capacitance, Resistance

MCL = Maximum Contaminant Level

MCLG = Maximum Contaminant Level Goal

MDL = Method Detection Limit

OH • = Hydroxyl Radical

PAHs = Polycyclic Aromatic Hydrocarbons

PRBs = Permeable Reactive Barriers

RMS = Root Mean Square

US EPA = the United States Environmental Protection Agency

LIST OF SYMBOLS

C = Concentration with time
C_o = Initial concentration
D = Diffusion coefficient
E = Electrical potential
f = AC frequency
F = Faraday's constant (= 96,487 C/mol)
j = Current density
j_{eqv} = Equivalent current density
J = Mass flux
k = Pseudo-first-order degradation rate constant
I_p = Peak current
I_{rms} = Root-mean-square current
R = Molar gas constant (= 8.314 kJ/mol-K)
T = Temperature
$t_{1/2}$ = Half-life
v = Linear velocity of solution
V_p = Peak voltage
V_{rms} = Root-mean-square voltage
z = Charge on a reacting species
Z = Impedance

CHAPTER ONE INTRODUCTION

1.1 OCCURRENCE OF PAHs IN WATER

Polycyclic aromatic hydrocarbons (PAHs) are a class of organic compounds that consist of two or more fused benzene rings and they are highly recalcitrant molecules that can persist in the environment due to their hydrophobicity and low solubility in water (Bamforth and Singleton 2005). According to the United States Environmental Protection Agency (USEPA 2006), PAHs similar to benzo(a)pyrene potentially cause health effects from acute exposure at levels above the maximum contaminant level (MCL) such as red blood cell damage leading to anemia and suppressed immune system. MCL is used as the drinking water standard in the U.S. MCL and maximum contaminant level goal (MCLG) of benzo(a)pyrene are 0 and 0.2 μg/L, respectively. This shows that extremely low concentration of PAHs can cause fatal diseases (USEPA 2006). It has been observed that that benzo(a)pyrene has the potential to cause cancer from lifetime exposure at levels above the MCL (USEPA 2006).

1.2 EXISTING REMEDIATION TECHNIQUES

Several techniques for remediation of contaminants including PAHs in water, soil, or sediments at the laboratory scale and at pilot or field scale have been investigated. These technologies are briefly described below.

1.2.1 Advanced Oxidation Processes (AOPs)

AOPs are based on the chemical, photochemical, and photo-catalytic production of hydroxyl radicals (OH*), which act as strong oxidant agents able to react with organics yielding dehydrogenated or hydroxylated derivatives. This radical is the main oxidizing agent of organic material, causing its mineralization, in other words, its conversion to CO₂, water, and inorganic ions (Louhichi *et al.* 2006). This method has major advantages, relatively high oxidation efficiency, fast reaction rate, and easy operation.

1.2.2 Permeable Reactive Barriers (PRBs)

A permeable reactive barrier (PRB) is defined as an *in situ* method for the remediation of contaminated groundwater. The PRB concept consists of reactive media such as zero valent iron, placed in the subsurface in the form of a vertical curtain through which the plume of contaminated groundwater moves and is treated (US EPA 1998). A PRB is a trap for contaminants where the barrier acts as a passive treatment system.

1.2.3 Membrane Processes

Membrane processes are modern physicochemical separation techniques that use differences in permeability (of water constituents) as a separation mechanism. Four types of pressure-driven membranes are currently used in municipal water treatment: microfiltration (MF), ultrafiltration (UF), nanofiltration (NF), and reverse-osmosis (RO) (Crittenden *et al.* 2005).

1.2.4 Electrokinetic Remediation

Electrokinetic remediation process typically removes heavy metals, anions, and polar organic contaminants from low permeability soil, mud, sludge, and marine dredging, using electrochemical and electrokinetic processes of desorption and removal. In other words, this *in situ* soil processing technology is primarily a separation and removal method for extracting contaminants by the means of electromigration.

1.2.5 Granular Activated Carbon (GAC) Adsorption

Granular activated carbon (GAC) adsorption is frequently used for the removal of hazardous organic pollutants from groundwater or wastewater. This technology achieves a rapid removal of the organic pollutants and retains them on the GAC surface (Caňizares et al. 2004).

1.3 OBJECTIVES

1.3.1 Key Challenges

Electrochemical degradation processes run at very high efficiency and operate essentially under the same conditions for a wide variety of waste (Grimm et al. 1998). Many researchers have reported lab-scale electrochemical degradation of organic compounds (Alshawabkeh and Saraheny 2005). However, there is lack of research on effects of scale on the rate of electrochemical degradation and power consumption. It would be vital to have such date if lab-scale data is to be used for the design of pilot-scale tests.

1.3.2 Target Contaminants

Two chemical compounds, naphthalene and salicylic acid, were selected to investigate in this study. Naphthalene, one of the model PAH compounds exists in soil, sediment, groundwater, and the atmosphere, and is naturally present in fossil fuels such as petroleum and coal. In addition, most naphthalene consumption (60%) is through its use as an intermediary in the production of phthalate plasticizers, resins, phthaleins, dyes, pharmaceuticals, and insect repellents. About 5% of naphthalene is released into water, primarily through coal tar production and distillation processes (ASTDR 1995). In other words, the widespread use and production of naphthalene in the United States is directly connected with the releases through various media and, furthermore, this inflow of naphthalene to the surface or the subsurface (e.g. to groundwater) is potentially threatening human health. According to Alshawabkeh and Sarahney (2005) and Goel et al. (2003), naphthalene has been used as a target contaminant because it has chemical and physical properties similar to other PAHs except that it is more soluble in water. This property of naphthalene makes its use attractive for lab-scale research.

Salicylic acid (2-hydroxybenzoic acid) is the key metabolite of various analgesics (e.g. aspirin) and is a common component in sewage effluent. Exposure of salicylic acid to human body can cause impacts to the central nervous system and the acid-base imbalance in the body, resulting in delirium and tremor, and dermatitis for the long and short-term (CDC 1997).

While the key objective of this study was to study the effect of scale on electrochemical degradation of naphthalene (a PAH), salicylic acid was also used to make up for these disadvantages of naphthalene: relatively low solubility, comparing

(0.0031g/100 mL for naphthalene versus 0.2 g/100 mL for salicylic acid); and its volatility as a function of temperature. In addition, salicylic acid dissociates into charged ions when mixed with water. The key physical and chemical properties of naphthalene and salicylic acid are presented in Table 1.1.

1.3.3 Key Objectives

The objectives of this study were to:

- Investigate the effect of current type and current density on electrochemical degradation of naphthalene and salicylic acid in an aqueous solution and sandy soil;
- Investigate the effect of scale of electrochemical cell on the rate of degradation and electrical power consumption; and
- Predict the change in concentrations during the test using the Nernst-Planck mass transport equation.

Table 1.1: Properties of naphthalene^a and salicylic acid^b

	Naphthalene	Salicylic Acid
IUPAC Name	Naphthalene	2-Hydroxybenzoic acid
CAS No.	91-20-3	69-72-7
ICSC No.	0667	0563
EINECS No.	202-049-5	200-712-3
Chemical Formula	C ₁₀ H ₈	C ₇ H ₆ O ₃
Chemical Structure		ОН
Molecular Mass (g/mole)	128.18	138.1
Appearance	White solid in various forms, with characteristic odor	Colorless crystalline powder or needle-shaped crystals
Melting Point (°C)	81.2	159
Boiling Point (°C)	218	211 (at 2666 Pa)
Flash Point (°C)	80	157
Vapor Pressure (Pa)	11 (at 25 °C)	114 (at 20 °C)
Density (g/cm³)	1.16	1.44 (at 20 °C)
Solubility in Water (g/100mL)	0.0031	0.2 (at 20 °C)
Octanol/ Water Partition Coefficient	3.3	2.2

Note: a CDC (2005), b CDC (1997)

CHAPTER TWO

ELECTROCHEMICAL DEGRADATION

2.1 DEGRADATION MECHANISM

During electrochemical degradation, the organic chemicals are destroyed or converted by either direct or indirect oxidation processes (Pepprah and Khire 2008). The schematic of these processes is illustrated in Figure 2.1 and discussed in the following sections.

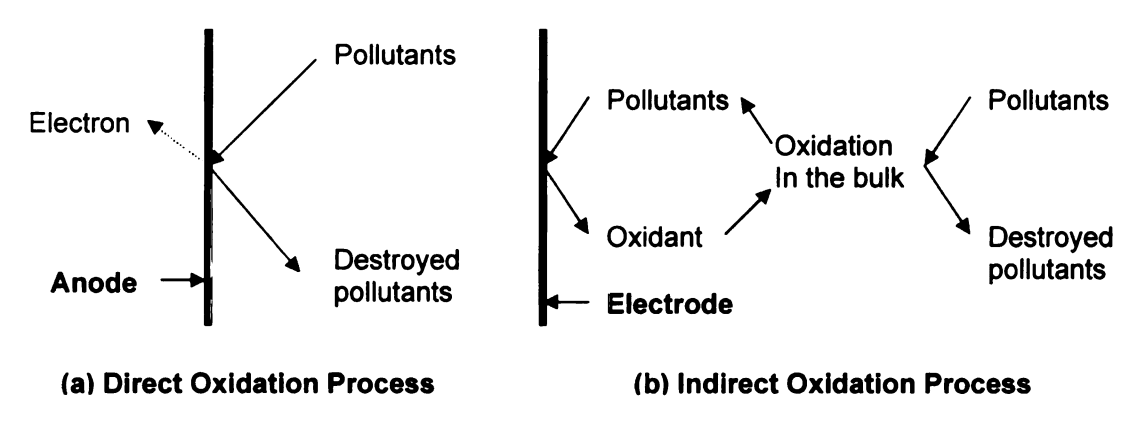


Figure 2.1: Schematic of pollutant removal pathways during electrochemical oxidation (Chiang et al. 1994)

2.1.1 Direct Electrolysis

During direct anodic oxidation [Figure 2.1 (a)], the chemicals are initially adsorbed on the surface of the anode where they are degraded by the anodic electron transfer reaction. Direct electrolysis methods include: anodic and cathodic processes.

Acar and Alshawabkeh (1996) suggested the following chemical reactions at the anode

and at the cathode, if the electrolytes are separated using a protonic membrane to prevent mixing but allow charge flow:

Anode:
$$2H_2 \rightarrow O_2 + 4H^+ + 4e^-$$
; $E^0 = +1.229 \text{ V}$ (2.1)

Cathode:
$$2H_2O + 2e^- \rightarrow H_2 + 2OH^-$$
; $E^0 = -0.828 \text{ V}$ (2.2)

2.1.2 Indirect Electrolysis

During indirect anodic oxidation [Figure 2.1 (b)], strong oxidants such as hypochlorite/ chlorine, ozone, or hydrogen peroxide are electrochemically generated. The pollutants are then degraded by the oxidation reaction with these strong oxidants. Among the oxidants, generation of hypochlorite is relatively common because a majority of the effluents contain chloride (Rajkumar *et al.* 2005). The chemical oxidation/reduction reactions of chlorine and hypochlorite are presented below:

Anode:
$$2Cl^{-} \rightarrow Cl_{2(g)} + 2e^{-}; E^{o} = -1.3583 \text{ V}$$
 (2.3)

Cathode:
$$2H_2O + 2e^- \rightarrow H_2 + 2OH^-$$
; $E^0 = -0.828 \text{ V}$ (2.4)

Bulk Solution:
$$Cl_2 + H_2O \rightarrow HOCl + H^+ + Cl^-$$
 (2.5)

$$HOCI \rightarrow H^{+} + OCI^{-}$$
 (2.6)

2.2 FACTORS AFFECTING ELECTROCHEMICAL DEGRADATION

Effect of concentration of electrolyte and electrode material, surface area, and size of electrodes, pH, and type of supporting electrolyte on the electrochemical degradation of pollutants have been presented in various studies (Wu et al. 2007). In this study, effect

of the size of the electrochemical cell for AC and DC application at various current densities was evaluated.

2.2.1 Electrode

Various types of electrodes have been used in the electrochemical degradation investigations and are introduced as follows.

- Titanium metal having dimensions: 5.0×3.5×0.1 cm, which was polished roughly
 (Wu et al. 2007 and Pepprah and Khire 2008);
- Titanium core with mixed metal coating having dimensions: 10.2×1.3×0.12 cm
 (Alshawabkeh and Sarahney 2005);
- Stainless steel plate as cathode and titanium mesh with a mixed metal oxide coating as anode having dimensions: 3.18×6.35×0.15 cm for both electrodes and distance between electrodes equal to 1.4 cm (Goel et al. 2003);
- Boron doped diamond electrode (BDD) as anode and a stainless steel plate as cathode, with an immersed area of 20 cm² (Carvalho et al. 2007);
- BDD anode, stainless steel cathode, and disks for both electrodes with a geometrical area of 50 cm² each and an inter-electrode gap of 1cm (Panizza et al. 2008); and
- Diamond-based material as anode, stainless steel as cathode, having circular shape (100 mm diameter) for both electrodes with geometric area of 78 cm² for each electrode and an electrode gap of 9 mm (Caňizares *et al.* 2005).

2.2.2 Supporting Electrolyte

2.2.2.1 Sodium Chloride (NaCl)

Alshawabkeh and Sarahney (2005) used sodium chloride (NaCl) as a supporting electrolyte for electrochemical degradation of naphthalene in aqueous solution and showed that generating Cl₂ (g) enhances the degradation of naphthalene in the solution. It is due to the formation of hypochloric acid. In addition, Panizza *et al.* (2005) have reported that the presence of hypochlorite, formed from the active chlorine electrochemically generated on the anode surface, must be related due to the oxidation of chloride ions when NaCl was used as a supporting electrolyte (Equation 2.3 to 2.6). However, post-treatment for the occurrence of chlorine should be considered as well as its efficiency in electrochemical remediation of organic compounds. Pepprah and Khire (2008) have reported faster decay and fouling of 99% pure titanium electrodes when NaCl instead of Na₂SO₄ was used as the supporting electrolyte.

2.2.2.2 Sodium Sulfate (Na₂SO₄)

Louhichi et al. (2006) used 1 M sodium sulfate (Na₂SO₄) as the supporting electrolyte in the electrochemical oxidation of benzoic acid on boron-doped diamond in aqueous solution. Furthermore, Feng and Li (2003) employed 0.25 M Na₂SO₄ as the supporting electrolyte to investigate the electro-catalytic oxidation of phenol (100 ppm) on titanium plated electrode with several metal-oxide electrodes, such as Sb-Sn-RuO₂-Gd, Sb-Sn-RuO₂, and RuO₂, in aqueous solution. Pepprah and Khire (2008) reported a lower degradation rate when Na₂SO₄ was used, compared to when NaCl was used as the supporting electrolyte. The key reason was for higher degradation rate when NaCl was

used as the supporting electrolyte was attributed to the formation of hypochlorite which acts as a strong oxidant.

2.2.3 Current Type

Chin and Cheng (1985) explored alternating voltage (AV) waveforms (sinusoidal, square, and triangular waves) where the frequency ranged from 20 to 6,000 Hz, and to determine the effect of AC on the oxidation of phenol using platinum electrodes in an aqueous H₂SO₄ supporting electrolyte. The electrolyte consisted of 0.01 to 0.1 M phenol in 1 M H₂SO₄ and platinum rotating disk having surface area of 12.5 cm² was immersed in the electrolyte contained in a 1 L Pyrex glass jar (undivided cell). The rate of conversion of phenol increased with increasing magnitude of the AC voltage and decreased with increasing AC frequency. Electric energy consumption was observed to be smaller than during DC electrolysis.

Nakamura *et al.* (2005) proposed the mechanism of decomposition of organic compounds based on selective redox reactions with various radicals generated by AC electrolysis that allows both oxidation and reduction in the same cell between adjacent electrodes. For this study, trichlorobenzene (TCB) solution (0.66 μM) containing NaOH or NaCl (20 mM) was selected as the supporting electrolyte. In addition, titanium plated electrodes having dimensions equal to 35×175×1 mm, the distance between neighboring electrodes was 25 mm, and contact area with electrolyte was 56 cm². The different radicals such as hydrogen atom (H*) and hydroxyl radical (OH*), generated by AC electrolysis, react with TCB, while having different pathways of decomposition.

2.2.4 Current Density

Sarahney and Alshawabkeh (2007) investigated the effect of current density on electrolytic transformation of benzene for groundwater remediation. By using 1, 5, and 10 mA DC that were converted to the current densities of 1.8, 9.0, and 18.2 mA/L, it was possible to indicate the amount of electric charge applied per unit volume of electrolyte and show that degradation rate is dependent on the current density.

2.3 INDEX OF EFFICIENCY

There are various indices used by researchers to evaluate the effect of various parameters related to the applied current. Based on the energy efficiency, the fate of the technology for potential field application can be assessed. These efficiency indices are as follows.

2.3.1 Instantaneous Current Efficiency (ICE)

The instantaneous current efficiency (ICE) of the electrolysis was calculated using the following relation introduced by Comninellis and Pulgarin (1991):

$$ICE (\%) = \frac{(COD_t - COD_{t+\Delta t})}{8I\Delta t} FV \times 100$$
 (2.7)

where $(COD)_t$ and $(COD)_{t+\Delta t}$ are the chemical oxygen demands at time t and $t+\Delta t$ (g/L); respectively; I is the current (A); F is the Faraday constant; V is the volume of electrolyte (L); and 8 is the equivalent mass of oxygen (g/eq).

2.3.2 Electrical Energy

As expressed in Eq. 2.8, electrical energy is consumed when current flows. This parameters expressed in the units of joule (J), watt (W), and watt-hour (Whr) are directly related with the operational cost and thus, will be a significant factor to determine both the applicability and efficiency of electrochemical degradation.

$$Power = Current \times Voltage \tag{2.8}$$

2.3.3 Pollutant Breakdown Rate per Charge

According to Alshawabkeh and Sarahney (2005), pollutant breakdown rate as a function of current density can be expressed as shown in Eq. 2.9:

$$rate = \frac{\Delta C / \Delta t}{i}$$
 (2.9)

where "rate" is the degradation rate of the pollutant (mg/L-hr); ΔC is the decrease in concentration (mg/L); Δt is the duration (hr); and j is the current density (mA/L or mA/cm²).

2.3.4 Electrical Efficiency (Long Order Reduction)

$$EE/O = \frac{P \times t}{V \times \log(C_i / C_f)}$$
 (2.10)

where EE/O is electrical efficiency as per long order reduction (kWh/m³); P is lamp power output, (kW); t is irradiation time (hours); V is reactor volume (m³); and C_i and C_f is initial and final concentration (mg/L), respectively.

2.4 MASS TRANSFER PROCESS: THE NERNST-PLANCK EQUATION

Mass transfer is the migration of mass from one location in solution to another and arises either from differences in electrical or chemical potential at the two locations or due to the mechanical movement (e.g. stirring or mixing) of the solution (Bard *et al.* 2001). The modes of mass transfer are defined by:

- Migration: movement of a charged body under the influence of an electric field (i.e. gradient of electrical potential);
- Diffusion: movement of a species under the influence of a gradient of chemical potential (i.e. a concentration gradient); and
- Convection: stirring or hydrodynamic transport. Fluid flow is divided by natural convection (convection caused by density gradient) and forced convection.

Equation 2.11 is the Nernst-Planck equation that simulates mass transfer due to migration, diffusion, and convection.

$$J_{i}(x) = -D_{i}(x)\frac{\partial C_{i}(x)}{\partial x} - \frac{z_{i}F}{RT}D_{i}C_{i}\frac{\partial \phi(x)}{\partial x} + C_{i}v(x)$$
 (2.11)

where $J_i(x)$ is the total flux of specie i (mol s⁻¹ cm⁻²) at distance x from the electrode surface; D_i is the diffusion coefficient (cm² s⁻¹); $\partial C_i(x)/\partial x$ is the concentration gradient at distance x; $\partial \phi(x)/\partial x$ is the potential gradient; z_i and C_i are the charge (dimensionless) and concentration (mol cm⁻³) of species i; respectively; and v(x) is the velocity (cm s⁻¹) with which a volume element in solution moves along the axis.

The Hayduk-Laudie relationship (1974) (Eq. 2.12) was used to estimate the diffusion coefficient for naphthalene and salicylic acid.

$$D = \frac{13.26 \times 10^{-5}}{\eta^{1.14} \times \overline{V}^{0.589}}$$
 (2.12)

where D is molecular diffusion coefficient (cm² s⁻¹); η is the solution viscosity in centipoises (10⁻² g/cm-s) at the temperature of interest; and V is the molar volume of the chemical (cm³/mol).

CHAPTER THREE EXPERIMENTAL METHODOLOGY

The overall experimental procedure is outlined in Figure 3.1. Each step is described in detail in the following sections.

Description

Name

Name		Description		
	Spiked Solution Preparation	Prepare 20 mg/L of naphthalene or salicylic acid. Add 5 mg/L of Na ₂ SO ₄ as supporting electrolyte.		
	Reaction Chamber Preparation	a. Prepare reaction vessel containing the pollutant sealed with Teflon cap. b. Put reaction vessel in water bath.		
		$\overline{\Box}$		
	Electrical Equipment Setup	a. Apply given current to the cell for given time period. b. Measure some parameters such as temperature, current, and voltage.		
	Sampling & Analysis	a. Take samples at specific elapsed times. b. Achieve the quantified concentrations with the aid of an HPLC c. Obtain the quantified concentrations from the analysis.		
		$\overline{\Box}$		
	Cleaning up & Recycling	Polish the electrodes used in the test. Wash sand and put it into oven over 48 hours at temperature of 80 °C.		

Figure 3.1: Schematic of testing procedure

3.1 EXPERIMENTAL SETUP

The experimental setup, as depicted in Figure 3.2, consists of reaction chamber, electrical equipment, and analytical instruments. Each constituent is specified and described below.

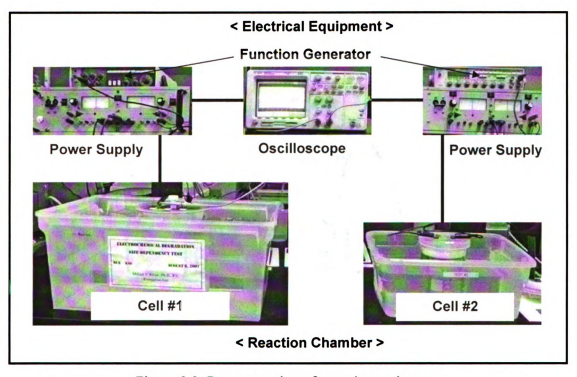


Figure 3.2: Representation of experimental setup

3.1.1 Reaction Chamber

The electrochemical degradation of naphthalene and salicylic acid was carried out in a single compartment (i.e. undivided cell) made of Pyrex glass beakers having 1 L or 4 L volumes, separately. The cell was capped with a Teflon cap. These materials (glass and Teflon) were selected to reduce or minimize sorption of contaminants onto to the walls of the reaction vessel as well as the cap. A water bath was used to prevent the cell from

Joule heating and, the room temperature was maintained at around 22 0 C. The picture of the reaction chamber immersed in the water bath is shown in Figure 3.3.

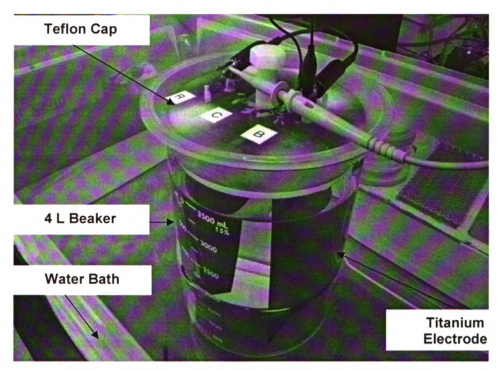


Figure 3.3: Picture of a reaction chamber for the 3.5 L Cell

3.1.1.1 Titanium Electrode

Titanium plate electrodes were used for this study. The titanium electrode used in this study were not coated. Uncoated titanium is cheaper than gold, platinum, or titanium coated with mixed metal oxides. Furthermore, titanium offers resistance to corrosion in wide range of aggressive conditions. In addition, titanium anodes are more stable than nickel, lead, zinc or mercury (Titanium Information Group 2002). Also, it is well known that titanium is easily reduced from Ti⁴⁺ to Ti³⁺ and acts as a charge carrier when an electric field is applied (Chen et al. 2003). For these reasons, it was thought that titanium is better a choice of electrode for this project. The purity of the titanium used was about

99%. For a smaller cell, each titanium electrode was 12 cm × 5 cm and the resulting area was 60 cm². However, area of the electrode immersed in the electrolyte was about 55 cm² and the spacing between adjacent electrodes was maintained at 8 cm. The dimensions of titanium electrodes for the two cells are presented in Figure 3.4 and Table 3.1. In addition to the plate, titanium screws and nuts were used as the current collector on both anode and cathode to minimize the reactivity of the current collectors and to reduce the possibility of corrosion due to a material difference.

3.1.1.2 Cell Volume (1 L Cell vs. 3.5 L Cell)

As mentioned in Chapter 1, one of the key objectives was to explore the effect of cell scale under same conditions except for the size of electrodes, the spacing between the two neighboring electrodes, and the resulting electrolyte volume participated in electrochemical reactions. To develop this, the Pyrex glass beakers having of 1 L and 4 L volume were selected and the electrolyte solution or other media was filled to 1 L (or 1,000 cm³) and 3.5 L (or 3,500 cm³), respectively. In this study, the former and the latter will be designated by 1 L cell and 3.5 L cell, respectively. These cells having different sizes, as depicted in Figure 3.5, can be characterized by physical and electrical parameters. The contact areas with electrolyte for the 1 L and 3.5 L cells are 55 and 178 cm², respectively (Table 4.1). Based on this data and the spacing between the electrodes (8 cm for 1 L cell, 9.5 cm for 3.5 L cell), the volume (area x spacing) participated in the electrochemical reactions was obtained and the resulting volumes for each cell were 440 and 1,691 cm³, respectively. This study started from the measures of degradation in the 1 L cell so that a volumetric ratio of volume of the 3.5 L cell to the 1 L cell (~3.854) could be used to determine the equivalent current density applied for the 3.5 L cell. To maintain the current density of 1 mA/cm² for the 1 L cell, the magnitude of the current was 55 mA. To maintain the current density of 1 mA/cm² for the 3.5 L cell, the magnitude of the current was 212 mA (\sim 55 mA X 3.85). In a similar manner, applied current for various j_{eqv} can be computed and the computations are presented in Table 3.2 and 3.3.

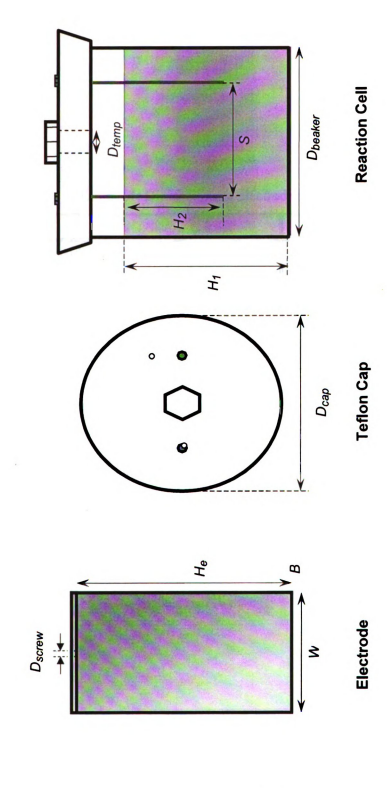


Figure 3.4: Schematic of the titanium electrodes, assembled cell, and Teflon cap

Table 3.1: Dimensions of electrodes, glass beaker, and Teflon cap

	1L Cell	3.5L Cell	Unit
1. Electrode			
Length (H _e)	11	19.2	cm
Width (W)	5	10.2	cm
Thickness (B)	1.63	1.55	mm
Diameter of Titanium Screw (D _{screw})	0.5	0.5	cm
2. Glass Beaker			
Depth of solution (H ₁)	12.5	19.5	cm
Immersed depth of electrode (H_2)	11	17.5	cm
Diameter of Bottom (D beaker)	11	16	cm
3. Teflon Cap			
Diameter of Cap (D_{cap})	13	19.5	cm
Diameter of temperature hole ($D_{temp.}$)	0.61	1.3	cm
Spacing between Electrodes (S)	8	9.5	cm

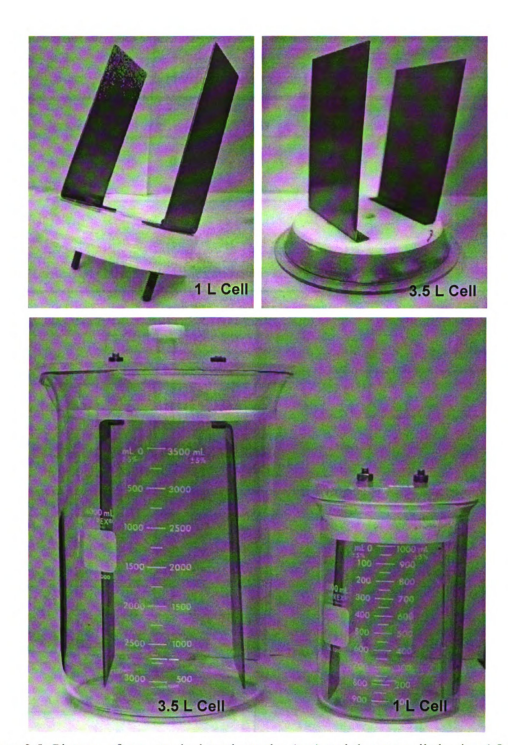


Figure 3.5: Pictures of cap attached to electrodes (top) and the two cells having 1 L and 3.5 L volume (bottom).

Table 3.2: Physical properties of 1 L and 3.5 L cells

Cell Type	Spacing (S, cm)	Area (A , cm²)	Treated Volume (V, cm ³)
1 L Cell	8	55	440
3.5 L Cell	9.5	178	1691

Table 3.3: Currents densities and equivalent currents for 1 L to 3.5 L cells

	Current aspec	cts for reaction cells	3					
	Current applied to	o electrodes (<i>i</i> , mA)					
Cell Type	$j_{eqv.}$ = 1 mA/cm ²	j _{eqv.} =2 mA/cm²	$j_{eqv.} = 3 \text{ mA/cm}^2$					
1 L Cell	55	110	165					
3.5 L Cell	212	424	636					
	Actual Current De	ensity (j _{actual} , mA/cı	m²)					
Cell Type	$j_{eqv.} = 1 \text{ mA/cm}^2$ $j_{eqv.} = 2 \text{ mA/cm}^2$ $j_{eqv.} = 3 \text{ mA/cm}^2$							
1 L Cell	1	2	3					
3.5 L Cell	1.19	2.38	3.57					
	Actual Current De	ensity (j _{actual} , mA/L)						
Cell Type	$j_{eqv.} = 1 \text{ mA/cm}^2$ $j_{eqv.} = 2 \text{ mA/cm}^2$ $j_{eqv.} = 3 \text{ mA/cr}$							
1 L Cell	125.00	250.00	375.00					
3.5 L Cell	125.37	250.74	376.11					

3.1.2 Electrical Equipment

The electrical equipment consisted of power supply, function generator, and oscilloscope (Figure 3.6). A 0 to 2 MHz sweep function generator was used to generate square wave form of AC. A square wave form was selected to equalize between root-mean-square voltage (V_{rmz}) and peak voltage (V_p) . Theoretically, a square wave form stays for half a cycle and shifts suddenly from negative to positive or vice versa. Thus, current with square wave form AC delivers greater power, compared to a sinusoidal or a triangular wave form of AC.

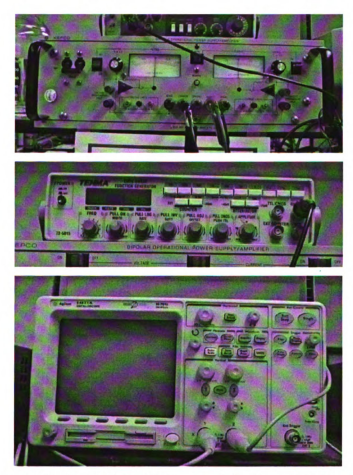


Figure 3.6: Pictures of electrical equipment used in the setup: power supply (top), function generator (middle), and digital oscilloscope (bottom)

The power supply consisted of a bipolar operational power supply/amplifier (Kepco) capable of producing up to 200 V AC/DC and 1 A AC/DC output or a maximum electrical power of 200 W. Values of electrical parameters such as voltage, current, and AC frequency were monitored by the aid of an oscilloscope (Agilent, 54621A).

3.1.3 Spiked Medium Preparations

3.1.3.1 Naphthalene in Aqueous Solution

Aqueous solutions, spiked with naphthalene, were prepared by adding naphthalene (EMD Chemicals Inc., 98% purity) crystals to deionized (DI) water in a Pyrex glass bottle and leaving it in a suspension for more than 72 hours. This was followed by the addition of supporting electrolyte to increase electrical conductivity. In this study, anhydrous Na₂SO₄ was used as the supporting electrolyte. The corresponding concentration of Na₂SO₄ was 500 mg/L (~ 3.5 mM) and this was based upon the MCLG of sulfate regulated by US EPA.

3.1.3.2 Salicylic Acid in Aqueous Solution

20 mg of salicylic acid purchased from EMD Chemicals Inc. (99% purity) was added to a 1 L Pyrex glass bottle containing DI water in order to have concentration of 20 mg/L. The addition of the supporting electrolyte follows the same procedure as that used for preparing the naphthalene solution.

3.1.3.3 Sand Spiked with Naphthalene or Salicylic Acid

For experiments with sandy soil spiked with naphthalene or salicylic acid, the solution prepared in steps described above was poured in 1,000 cm³ (or 3,500 cm³) of dry

Ottawa sand in 1 L (or 4 L) Pyrex glass beaker until full saturation of the sand was reached. It was presumed that the spiked sand was fully saturated when the surface of the solution rose above the sand surface.



Figure 3.7: Pictures of materials used in spiked medium preparations

3.1.4 Stirring Apparatus

A magnetic stirrer was used to continuously stir the solutions in reaction vessels (Fig. 3.8). The rate of the rotating magnetic bar was maintained at 1,200 rpm for both 1 L and 3.5 L cells. Depending upon the size of the reaction cell, magnetic bar having an appropriate length was used.

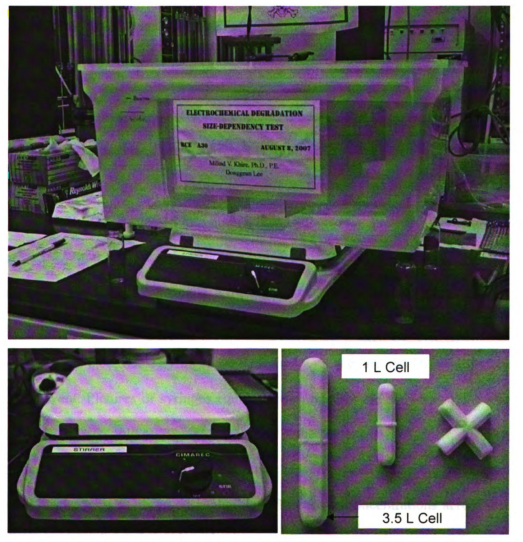


Figure 3.8: Pictures of stirrer with 3.5 L cell (top), stirrer (bottom, left), and magnetic bars (bottom, right)

3.2 TESTING, SAMPLING, AND ANALYZING TECHNIQUES

3.2.1 Sampling Technique

3.2.1.1 Sampling Frequency

During tests, samples were taken for high performance liquid chromatography (HPLC) analyses at time intervals equal to 0, 1, 2, 4, 8, and 24 hours for salicylic acid tests and 0, 1, 2, 4, 8, 24, and 48 hours for naphthalene tests.

3.2.1.2 Sampling Method

While the electrical current was applied, the test was not paused during sampling and samples were collected using syringes (Hamilton Co.) equipped with spiral needles (Popper & Sons, Inc.) having length appropriate for the size of the cell. After each sampling event, it was injected into amber vials (Supelco Co.) capped with a membrane (Supelco Co.), and then directly kept in a refrigerator for HPLC analyses. Needles with different lengths for different cells were determined and customized in order to take samples in the center of the volume that participated in the electrochemical degradation between the two electrodes. Syringes were cleaned with acetone and DI water before any sampling event. Pictures of syringes equipped with needles are shown in Figure 3.9. In aqueous phase tests, only one sample was taken in the center between electrodes. Pepprah and Khire (2008) have shown that the solution is well-mixed within the treated volume between electrodes and observed negligible difference in concentrations across the cell. Unlike aqueous phase tests, samples were collected three times at different three positions in the soil phase tests: one in the center between the electrodes, and one each in the vicinity of the two electrodes.

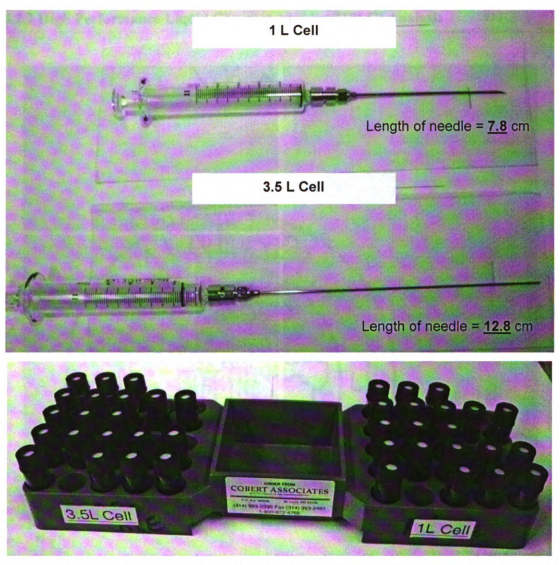


Figure 3.9: Pictures of syringes equipped with needles of different lengths (top) and amber vials with caps used for HPLC analyses (bottom)

3.2.2 High Performance Liquid Chromatography (HPLC) Analysis



Figure 3.10: Pictures of HPLC instrument

Concentrations of naphthalene and salicylic acid were measured using high performance liquid chromatography (HPLC). A Perkin-Elmer[®] system equipped with a tunable UV detector (detection at 254 nm), a Waters C-18 PAH, 250 mm×4.6 mm×5 µm column, an automated gradient controller, and deionized (DI) water/ acetonitrile mobile phase. The flow rate of the mobile phase was 1.2 mL/min and the column was flushed with 10:90 (v/v) acetonitrile/ DI water for 5 minutes followed by 60:40 (v/v) acetonitrile/ DI water for 10 minutes and by 100:0 (v/v) acetonitrile/ DI water for 5 minutes. This gradient was used for the analysis of naphthalene and salicylic acid in order to obtain

appropriate separation of the degradation product peaks on the chromatograms during the tests. These instruments can be seen in Figure 3.10.

Table 3.4: Preparation of standard solutions for naphthalene and salicylic acid

Volume of 1000 mg/L of Stock Solution	Volume of Acetonitrile	Concentration in Acetonitrile Solution
(μ L)	(mL)	(mg/L)
10	4	2.49
30	4	7.44
50	4	12.35
70	4	17.2
100	4	24.39
150	4	36.14

^{*} Note: DI water was used to make standard solutions for salicylic acid.

As shown in Table 3.4 above, standard solutions were prepared to bracket the expected concentration level of the analytes. The identification of naphthalene and salicylic acid was achieved by comparison of retention times to those of the respective standards. R^2 values in the resulting calibration curves were observed by the range of 0.998 to 0.999.

3.2.3 Duplicate Sampling

Most of the experiments were repeated to confirm changes in concentrations of naphthalene and salicylic acid existing in aqueous or sandy soil phase at a given elapsed time. When an experiment was repeated, total four analyses were conducted for each sampling round by HPLC because each sample is analyzed twice by the HPLC.

3.3 MONITORED EXPERIMENTAL PARAMETERS

Distinct from taking samples from the cells and obtaining concentrations of naphthalene and salicylic acid, other experimental parameters were also monitored. These parameters included temperature, pH, electrical conductivity, and standard redox potential monitored at given initial and final time elapsed. A portable dissolved oxygen/pH meter, equipped with a Platinum Series pH electrode was used to measure pH of the solution. A portable electrical conductivity meter (Oakton, Con 5 acon series) and a microprocessor thermometer (Omega, model HH21) were used to measure electrical conductivity and temperature within the cell, respectively. These measuring devices are displayed in Figure 3.11.



Figure 3.11: Pictures of measuring devices

3.4 RECYCLING SOILS AND ELECTRODES

3.4.1 Soil Recycling

Soil washing is a water-based process that uses a combination of particle size separation and aqueous chemical separation to reduce contaminant concentrations in soil (US EPA 2007). Soil washing is effective on homogeneous, relatively simple contaminant mixtures in terms of its applicability and effectiveness. For the sandy soil phase experiments, Ottawa sand was used as a single media spiked with naphthalene or salicylic acid and hence, this method could be suitable for contaminant removal and soil recycling.

This process is specifically described below and illustrated in Figure 3.12:

- Step 1: clean the container using acetonitrile and DI water.
- Step 2: dump used sand into the container after the test is finished.
- Step 3: fill DI water in the container.
- Step 4: stir the "contaminated" sand and solution by the means of a steel rod gently and repeat this step for 4 times.
- Step 5: transfer washed sand to an aluminum tray.
- Step 6: put the tray containing sand and water into a hot air oven maintained at a temperature of 80 °C for over 48 hours.

In order to verify the effectiveness of this method, the HPLC analysis was followed by taking samples after each washing event covering Step 3 and 4 and the spiked chemicals were not detected in the washed Ottawa sand.

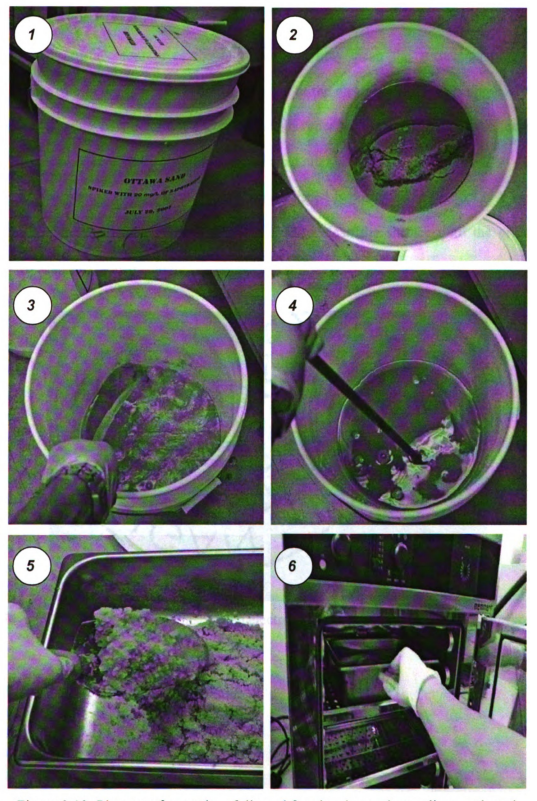


Figure 3.12: Pictures of procedure followed for cleaning and recycling used sand

3.4.2 Electrode Recycling

The surface texture of the electrode and how clean the surface is plays an important role in the rate of reactions that occur at the electrode surface (Pepprah 2007). Instead of using new electrode for each test, in order to lower the cost of the project, electrodes were re-used by cleaning and polishing after each test.

The picture of how the electrode was polished is presented in Fig. 3.13. A metal brush grinder operated pneumatically was used to clean the surface until the original electrode surface was restored.

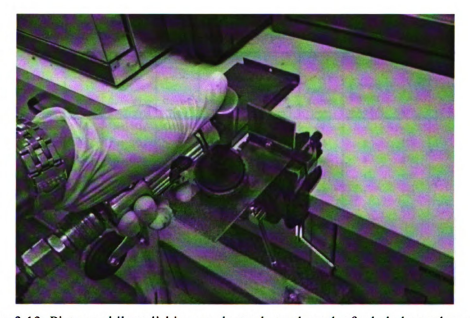


Figure 3.13: Picture while polishing an electrode to clean the fouled electrode surface

CHAPTER 4 RESULTS AND DISCUSSION

The results of the electrochemical degradation experiments carried on spiked solutions of naphthalene and salicylic acid in an aqueous solution and in saturated sandy soil are presented in this chapter.

4.1 AQUEOUS PHASE EXPERIMENTS

The aqueous phase experiments carried out are summarized in Table 4.1

Table 4.1: Summary aqueous phase experiments

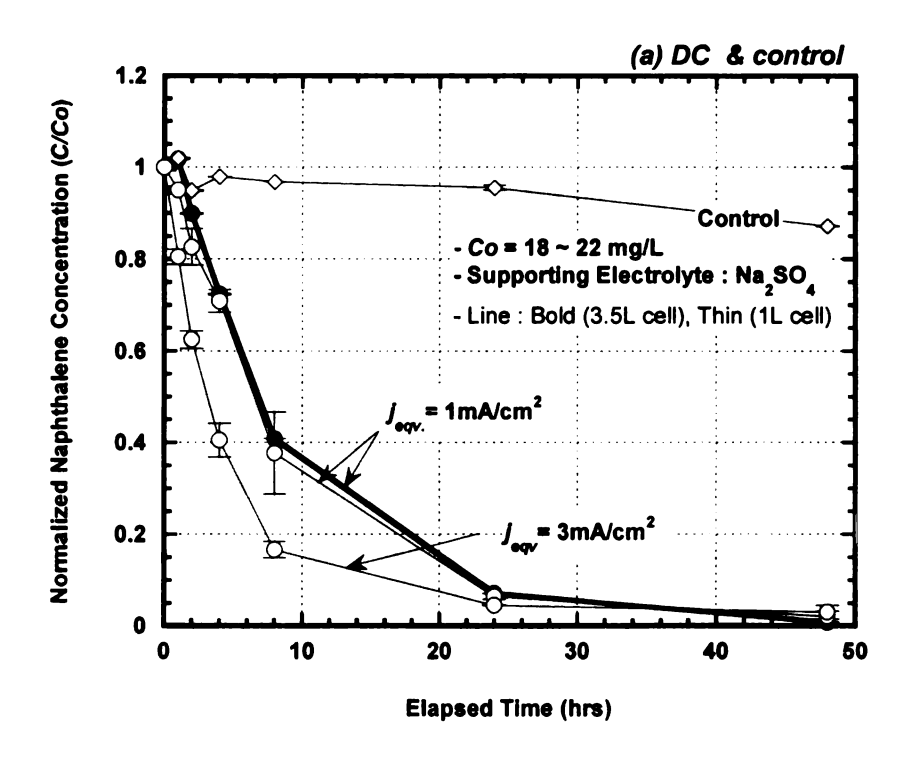
Compound	Medium	Cell Type	Supporting Electrolyte	Current Type	AC Frequency (Hz)	Equivalent Current Density (mA/cm ²)	Applied Current (mA)	Current Current Density (mA/cm ²)	Density (mA/L)	Stirring	Number of Tests
Naphthalene	Solution	1 L	Na ₂ SO ₄	Control	-	-	-	-	-		2
Naphthalene	Solution	1 L	Na ₂ SO ₄	AC	0.1	1	55	1	125	1	1
Naphthalene	Solution	1 L	Na ₂ SO ₄	AC	0.1	3	165	3	375		2
Naphthalene	Solution	1.L	Na ₂ SO ₄	AC	60	. 1	55	1	125		1
Naphthalene	Solution	1L	Na ₂ SO ₄	DC	0	1	55	1	125		2
Naphthalene	Solution	1 L	Na ₂ SO ₄	DC	0	3	165	3	375		2
Naphthalene	Solution	3.5 L	Na ₂ SO ₄	AC	0.1	1	212	1.19	125.37		1
Naphthalene	Solution	3.5 L	Na ₂ SO ₄	AC	0.1	3	636	3.57	376.11		100
Naphthalene	Solution	3.5 L	Na ₂ SO ₄	AC	60	1	212	1.19	125.37	1000	1
Naphthalene	Solution	3.5 L	Na ₂ SO ₄	DC	0	1	212	1.19	125.37	-	1
Salicylic Acid	Solution	1 L	Na ₂ SO ₄	Control	the de-	L cell,	teathing	W88 63	CENSIV	E Her	2
Salicylic Acid	Solution	1 L	Na ₂ SO ₄	Control			-			Y	1
Salicylic Acid	Solution	11	Na ₂ SO ₄	AC	0.1	300	165	3	375	s tem	2
Salicylic Acid	Solution	1 L	Na ₂ SO ₄	DC	0	1	55	1	125		1
Salicylic Acid	Solution	Int L	Na ₂ SO ₄	DC	0	3 0	165	3 3 Sul	375	prose	2
Salicylic Acid	Solution	1 L	Na ₂ SO ₄	DC	0	3	165	3	375	Y	2
Salicylic Acid	Solution	3.5 L	Na ₂ SO ₄	AC	0.1	3	636	3.57	376.11	Control of	2
Salicylic Acid	Solution	3.5 L	Na ₂ SO ₄	AC	0.1	3	636	3.57	376.11	Y	1
Salicylic Acid	Solution	3.5 L	Na ₂ SO ₄	DC	0	71	212	1.19	125.37	100	2
Salicylic Acid	Solution	3.5 L	Na ₂ SO ₄	DC	0	3	636	3.57	376.11	100	1
Salicylic Acid	Solution	3.5 L	Na ₂ SO ₄	DC	0	3	636	3.57	376.11	Y	1
								Total n	umber of	tests :	25

4.1.1 Naphthalene

Figure 4.1 shows the average normalized concentration (C/C_o) of naphthalene versus elapsed time for the test cells where DC and AC (peak) current densities of 1 and 3 mA/cm² was applied. Data for control cell is also presented for which no current was passed. All experiments were carried out with Na₂SO₄ as the supporting electrolyte. As presented in Chapter 3, equivalent current density (j_{eqv}) of 1 mA/cm² converts to 55 and 212 mA current applied to the 1 L and 3.5 L cells, respectively. j_{eqv} of 3 mA/cm² converts to 165 and 636 mA current applied to the 1 L and 3.5 L cells, respectively. The error bars shown in all plots presented in this chapter represent the maximum and minimum values of C/C_o obtained from all tests, including the replicate tests.

4.1.1.1 Effect of Current Density on Naphthalene Degradation

When DC having j_{eqv} of 1 mA/cm² was passed through the 1 L and 3.5 L cells, about 60% decrease in naphthalene concentration was observed within 24 hours. Whereas, when DC having j_{eqv} of 3 mA/cm² was passed, about 75% reduction in the concentration of naphthalene was observed within 8 hours for the 1 L cell. When DC having j_{eqv} of 3 mA/cm² was applied to the 3.5 L cell, heating was excessive. Hence, due to significant volatilization potential of naphthalene, the experiment was terminated. Instead, similar test was done with salicylic acid and the results are presented in subsequent sections of this chapter. The control cell showed relatively small loss in naphthalene, which is believed to be due to volatilization of naphthalene that can occur at room temperature.



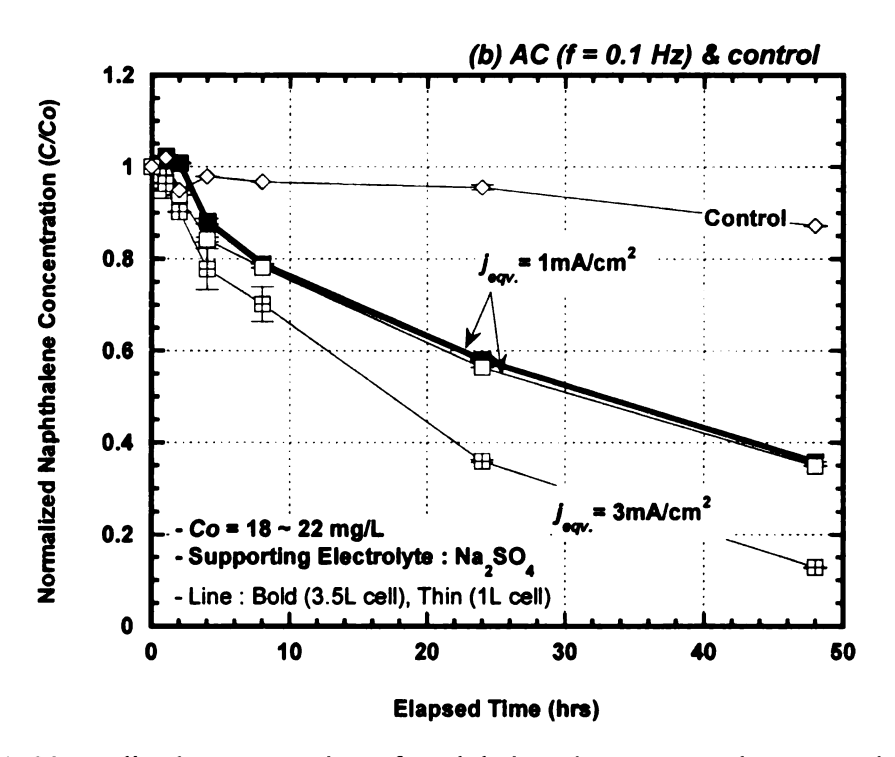


Figure 4.1: Normalized concentration of naphthalene in aqueous phase experiments for DC (a); and AC (f = 0.1 Hz) (b) performed at j_{eqv} of 1 and 3 mA/cm² in 1 L and 3.5 L cells

All other parameters being constant, for higher current density ($j_{eqv.} = 3 \text{ mA/cm}^2$), the observed degradation rate was greater than that for the lower current density ($j_{eqv.} = 1 \text{ mA/cm}^2$) regardless of the size of the cell. This finding is consistent with the results of Alshawabkeh and Sarahney (2005) and Pepprah and Khire (2008). For these tests, it was presumed that the electrode fouling did not happen at the electrodes for the time duration of 48 hours or it occurred at the same rate for various current densities. However, higher current densities would not guarantee a high current efficiency. Rodgers *et al.* (1999) reported that the current efficiency was consistently higher at low current densities because the positive polarization of the anode increases with current density and hence a greater fraction of the applied current is wasted in the electrolysis of water.

4.1.1.2 Effect of Current Type (AC vs. DC) on Naphthalene Degradation

In the DC application for j_{eqv} equal to 1 mA/cm² in the 1 L and 3.5 L cells, almost 90% reduction in naphthalene concentration was observed within 24 hours in both cells. However, only 45% reduction in the concentration was observed when AC (f = 0.1 Hz) having an equivalent current density equal to 1 mA/cm² was applied. Pepprah and Khire (2008) have attributed this due to the reversal in current direction during AC causing delay in mass transfer of naphthalene to the anode where it is oxidized. This results in a slower rate of degradation even if both electrodes (referred to as instantaneous anodes) participate in the oxidation when AC is used.

4.1.1.3 Effect of Size of Reaction Cells on Naphthalene Degradation

While the current passed through the 1 L and 3.5 L cells was different (55 mA for 1 L cell and 212 mA for 3.5 L cell for j_{eqv} equal to 1 mA/cm²), the shape and the rate of

degradation are very close for the two cells having different sizes for both AC and DC applications (compare bold and thin lines in Fig. 4.1). However, the rate of degradation was slightly greater for the 3.5 L cell. These results indicate that the size of the cell plays a relatively minor role for controlling the rate of degradation as long as the equivalent current densities are the same.

4.1.1.4 Degradation Kinetics

The degradation rate of naphthalene in aqueous solution during the electrochemical test could be described as a *pseudo*-first-order reaction (decay) that follows Equation 4.1.

$$\frac{dC}{dt} = -k[C] \tag{4.1}$$

where dC/dt is the rate of change of concentration with time; C is the concentration of naphthalene (mg/L); and k is the pseudo-first-order degradation rate constant (hr⁻¹).

$$t_{1/2} = \frac{\ln(2)}{k} = \frac{0.693}{k} \tag{4.2}$$

A plot of $\ln[C/C_o]$ yields k based on Eq. 4.2. The observed *pseudo*-first-order rate constant (k), the R^2 value, and the corresponding half-life $(t_{1/2})$ obtained from Equation 4.2 for the initial 24 hours for all experiments plotted in Fig. 4.1 are presented in Table 4.2 and plotted in Fig. 4.2.

Table 4.2 and Fig. 4.2 show that k increases and $t_{1/2}$ decreases when the equivalent current density is increased from 1 to 3 mA/cm² for the 1 L and 3.5 L cells. Table 4.2 also

shows that the size of the cell has minor influence on the k and $t_{1/2}$ values for a given current density.

Table 4.2: Degradation rate constant (k) and the corresponding half-life $(t_{1/2})$ for naphthalene tests in aqueous solution (time period = 24 hours)

			1L cell		3.5L cell			
Current Type	<i>j_{eqv.}</i> (mA/cm²)	<i>k</i> (hr ⁻¹)	R²	t _{1/2} (hr)	<i>k</i> (hr ⁻¹)	R²	t _{1/2} (hr)	
DC	1	0.117	0.997	5.9	0.114	0.997	6.1	
	3	0.126	0.939	5.5	-		-	
AC	1	0.023	0.978	29.9	0.024	0.964	29.0	
(f = 0.1 Hz)	3	0.042	0.993	16.5	-		-	

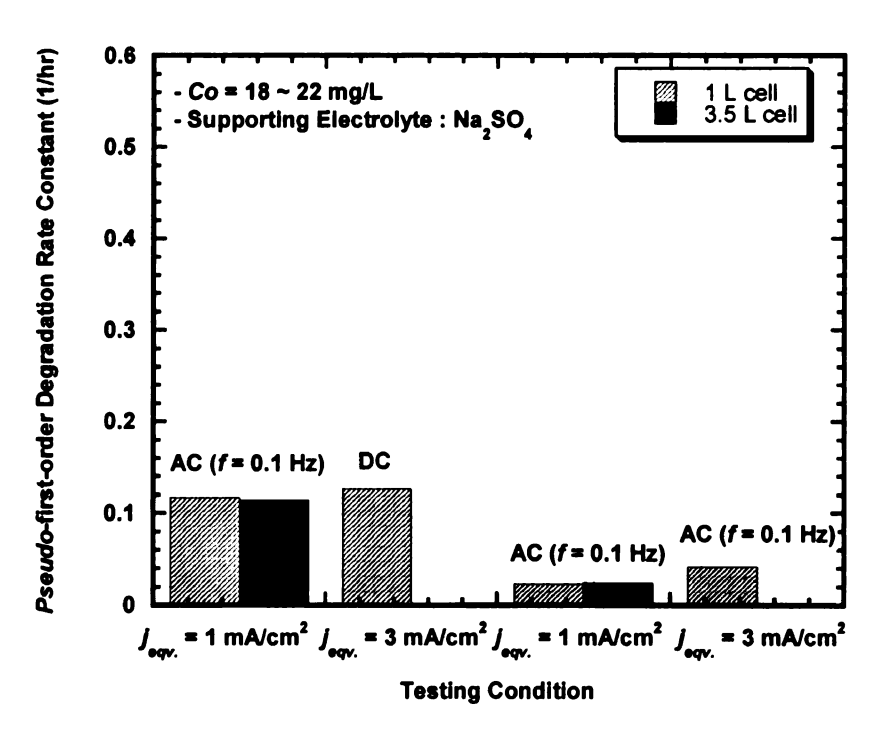


Figure 4.2: Estimated k from electrochemical degradation of naphthalene in aqueous solution

4.1.1.5 Cumulative Electrical Energy Consumption

Figure 4.3 shows the cumulative electrical energy consumed during the electrochemical degradation of naphthalene for the AC and DC tests when j_{eqv} of 1 mA/cm² was applied. During the application of DC, about 835 and 1,110 kJ/L of electrical energy was consumed in the 1 L and 3.5 L cells during the test duration of 48 hours, respectively. When AC was used (f = 0.1 Hz), about 210 and 320 kJ/L of electrical energy was consumed in the 1 L and 3.5 L cells during the test duration of 48 hours, respectively. While the power consumption for the AC tests was less than that for the DC tests, AC resulted in about 65% reduction in the concentration and DC resulted in about 95% reduction. The normalized power consumption for the 3.5 L cell was about 30% and 50% more than the 1 L cell for DC and AC application, respectively. The power consumption for the larger cell was more because the resistance (DC application) and impedance (AC application) of the larger cell was greater than the smaller cell. Hence, it required greater current which resulted in greater power consumption.

The 2008 cost for electricity generation is about U.S.\$ 0.065/kW-hr (source: Energy Information Administration). Table 4.3 presents the electricity cost (based on electricity generation only) for the 1 L and 3.5 L experiments carried out in this project. The volume of liquid that was between the two electrodes in each of the two cells (440 cm³ for the 1 L cell and 1,691 cm³ for the 3.5 L cell) was used for the cost calculation. This volume was believed to have participated in the electrochemical reactions. Table 4.3 shows that the electricity consumption cost increased five times when the cell size increased by about four times.

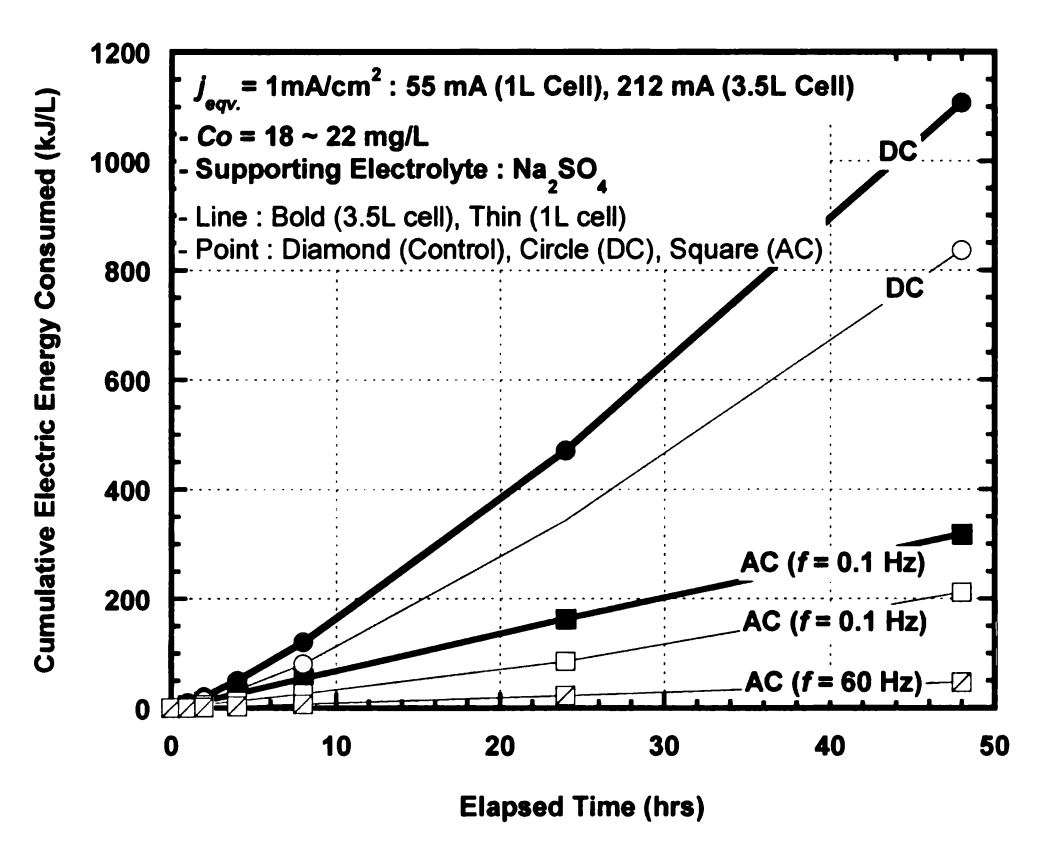


Figure 4.3: Cumulative normalized electric energy consumed during electrochemical degradation of naphthalene in aqueous phase experiments for DC and AC (f = 0.1 Hz) performed at j_{eqv} of 1 mA/cm² in 1 L and 3.5 L cells

Table 4.3: Comparison of electric energy consumption costs for 1 L and 3.5 L cells

	AC	Equivalent Current		Cumu	lative Electric I (at t = 48 hrs)	٠,			
Current Type	Frequency (Hz)	Density (mA/cm ²)	Cell Type	(kJ/L)	(kJ)	(kWh)	Cost (USD)	Cost Ratio (3.5 L / 1 L)	
AC	0.1	1	1 L	211.35	92995.65	25.85	1.68		
			3.5 L	317.95	537661.89	149.47	9.72	5.8	
DC	0	1	1 L	836.01	367844.40	102.26	6.65	-,	
			3.5 L	1107.58	1872916.67	520.67	33.84	5.1	

Note: The end-use prices of electricity in industrial sector are 6.5 cents per kilowatt-hour. The value of 0.000278 was used to convert the units from kilo joule to kilowatt-hour.

4.1.1.6 Measured Initial and Final Test Parameters

Table 4.4 summarizes the measured initial and final values of temperature, pH, standard redox potential, and electrical conductivity of the solutions in both the control and the test cells. These parameters are discussed below.

Temperature

A water bath was used to eliminate the degradation or volatilization of chemical compounds from *Joule* heating due to the electricity. All cells (including the control cell) were placed in a water bath. Heat generated in the test cells due to *Joule* heating was removed by the water bath and hence temperature within the cells stayed in the range of 19 to 23 0 C. At the final measurement (t = 48 hr), temperatures observed in the 3.5 L cell was higher than in the 1 L cell due to the application of approximately four-times greater current. The temperature in the 3.5 L cell was similarly controlled with the 1 L cell by using a relatively large water bath where the 4 L glass beaker was immersed to the top.

■ pH

The initial pH values ranges from 5.6 to 6.5. The final pH values measured after the test period (t = 48 hr) ranged from 3.8 to 4.5 in the AC test cells and from 6.5 to 11.5 in the DC test cells, respectively. From the water electrolysis, the oxidation of water molecules produces H⁺ at the anode while the reduction of water molecules generates OH⁻ ions at the cathode. In addition, formation of intermediate byproducts containing acidic substances may cause possible source of H⁺ ions in the solution. For the AC tests, full degradations of naphthalene were

not reached at the final elapsed time. Consequently, H⁺ ions from the oxidation of water molecule was probably more prominent in the AC tests and made the pH values decrease. In contrast, the DC tests show an increase in pH values as the test was completed (48 hr). In other words, indicating that the reduction of water molecules was more prominent as the test progressed.

Redox Potential

The standard redox potential values measured at the beginning of the experiment for all AC test cell solutions were generally higher than those at the final elapsed time.

Electrical Conductivity

The electrical conductivity values measured at the initial elapsed time are similar to those measured at the final elapsed time except for the DC tests. For the DC tests, there was a slight increase in the electrical conductivity.

Table 4.4: Summary of key physical parameters for naphthalene tests in aqueous solution

		Equivalent		Tempé	Temperature			Standar Pote	Standard Redox Potential	Elec	Electrical Conductivity
		Current		ಲ 	၂ (၃)	۵	됩	ב	(m)	Stl)	(μS/cm)
Cell	Current	Density	Current	initial	final	initial	final	initial	final	initial	final
Type	Туре	(mA/cm²)	(mA)	(t=0hr)	(t=48hrs)	(t=0hr)	(t=0hr) (t=48hrs)	(t=0hr)	(t=0hr) (t=48hrs)	(t=0hr)	(t=48hrs)
1 L	Control	0	0	19.2	19.0	6.5	6.5	394	422	811	810
1 L	DC	1	22	19.2	17.7	6.5	11.2	446	193	838	1135
1 L	DC	3	165	19.2	22.7	6.5	11.5	447	177	838	1172
1 L	AC (0.1Hz)	1	22	19.4	18.4	5.6	4.0	409	419	831	853
1 L	AC (0.1Hz)	3	165	19.2	18.0	6.5	4.5	394	415	811	818
3.5 L	DC	1	212	19.8	21.1	5.7	6.5	407	408	831	905
3.5 L	AC (0.1Hz)	1	212	19.5	18.8	5.8	3.8	356	405	800	843

4.1.2 Salicylic Acid

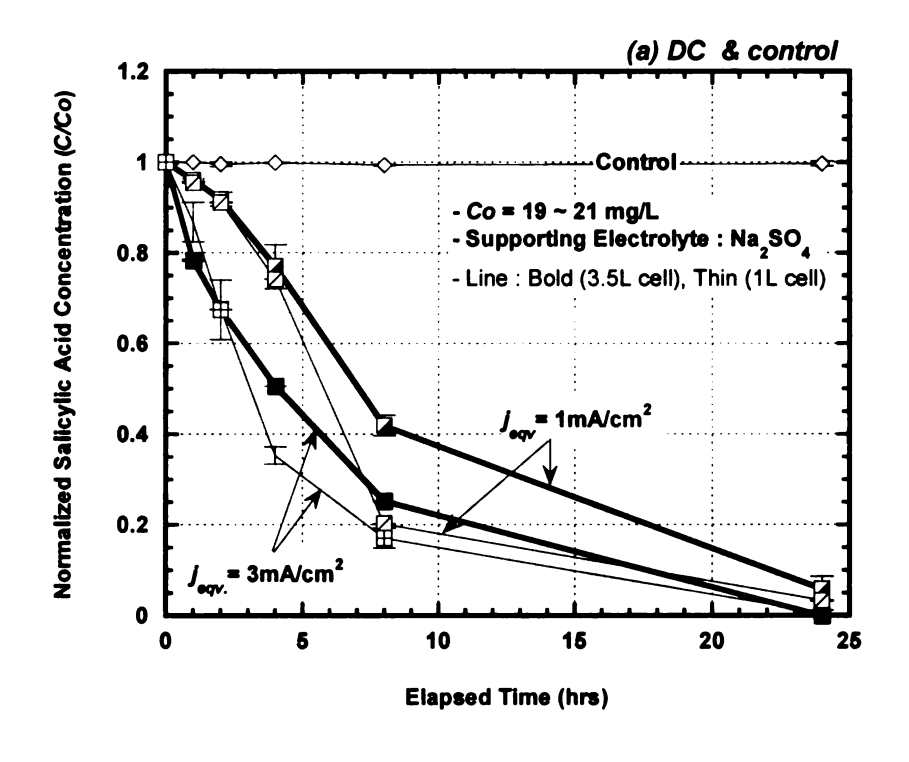
Figure 4.4 shows the average normalized concentration (C/C_o) of salicylic acid versus elapsed time for the experiments where salicylic acid was used as the target chemical for the experiments with 1 L and 3.5 L cells. The current densities used for AC and DC applications were 1 and 3 mA/cm² which is consistent with the naphthalene experiments. Na₂SO₄ was used as the supporting electrolyte similar to the naphthalene experiments.

4.1.2.1 Effect of Current Density on Salicylic Acid Degradation

When the 1 L and 3.5 L cells were subjected to j_{eqv} of 1 mA/cm² and 3 mA/cm² in DC application, the rate of degradation for the 3.5 L cell was more for higher current density application (Fig. 4.4a). However, for the 1 L cell, the increase in current density resulted in a greater increase in the rate of degradation only during the first 8 hours of the experiment. This is because the concentration reduced by 80% in the first hour and being a first order decay, the rate slowed down after 8 hrs.

4.1.2.2 Effect of Current Type (AC vs. DC) on Salicylic Acid Degradation

The 1 L and 3.5 L cells were subjected to j_{eqv} of 3 mA/cm² (636 mA) with DC and AC (f = 0.1 Hz, square wave) applications. The rate of degradation for the DC experiment was much higher (about 3 fold) than that when AC was used. This finding is consistent with the results of Pepprah and Khire (2008) and the results for naphthalene presented in previous sections.



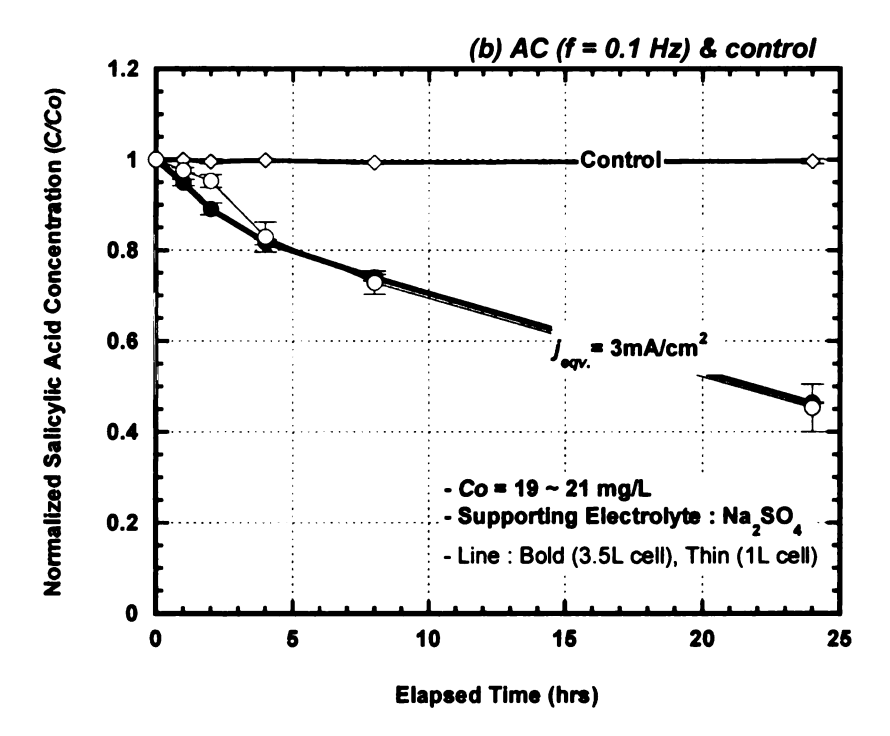


Figure 4.4: Normalized concentration of salicylic acid in aqueous phase experiments for DC (a) and AC (f = 0.1 Hz) (b) performed at j_{eqv} of 1 and 3 mA/cm² in the 1 L and 3.5 L cells

4.1.2.3 Effect of Scale of Cells on Salicylic Acid Degradation

For the DC application when j_{eqv} . Equal to 1 and 3 mA/cm² were applied, the rates of degradation for the 1 L cell was higher compared to the 3.5 L cell during the first 8 hours of the experiments. However, the rates were about the same after 8 hrs. For the AC application, for j_{eqv} equal to 3 mA/cm², the rate of degradation for both cells were about the same. While the current densities were the same for these cells, the ratio of surface area of the electrode in contact with the electrolytes to the volume of the electrolyte was higher for the 1 L cell. All reactions primarily occur at the electrode surface. This may be the reason why in DC tests the smaller cell showed faster rate of degradation. During AC tests, the surface area ratio does not dominate because the mass transfer to the electrodes is slowed due to the constant change in the direction of the current.

4.1.2.4 Degradation Kinetics

The plots of $\ln(C/C_o)$ versus time yield the *pseudo*-first-order reaction (decay) similar to that for naphthalene tests discussed previously. The degradation rate constant (k) of salicylic acid and the corresponding half-life $(t_{1/2})$ in the electrochemical application could be calculated using Equations 4.1 and 4.2, respectively. The values of k, R^2 , and $t_{1/2}$ obtained for the tests are summarized in Table 4.5 and plotted in Fig. 4.5.

Table 4.5: Degradation rate constant (k) and the corresponding half-life ($t_{1/2}$) for salicylic acid tests in aqueous solution (time period = 24 hours)

			1L cell		3.5L cell			
Current Type	j _{eqv.} (mA/cm²)	<i>k</i> (hr ⁻¹)	R²	t _{1/2} (hr)	<i>k</i> (hr ⁻¹)	R²	t _{1/2} (hr)	
DC	1	0.148	0.966	4.7	0.122	0.995	5.7	
	3	0.216	0.998	3.2	0.167	0.996	4.1	
AC	3	0.033	0.989	20.9	0.031	0.990	22.4	

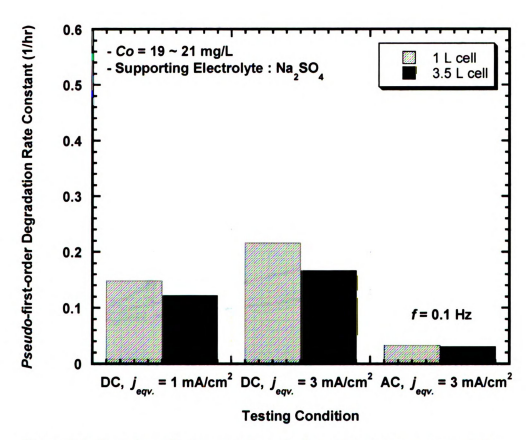


Figure 4.5: Variation of k observed for salicylic acid tests in aqueous solution

4.1.2.5 Cumulative Electrical Energy Consumption

The normalized cumulative electric energy (energy per unit volume of the electrolyte) consumed during the degradation of salicylic acid in aqueous solution is presented in Figure 4.6. For all current densities, the normalized electrical energy consumption for the 3.5 L cell was much greater than that for the 1 L cell. These results are similar to those when naphthalene was used as the target contaminant.

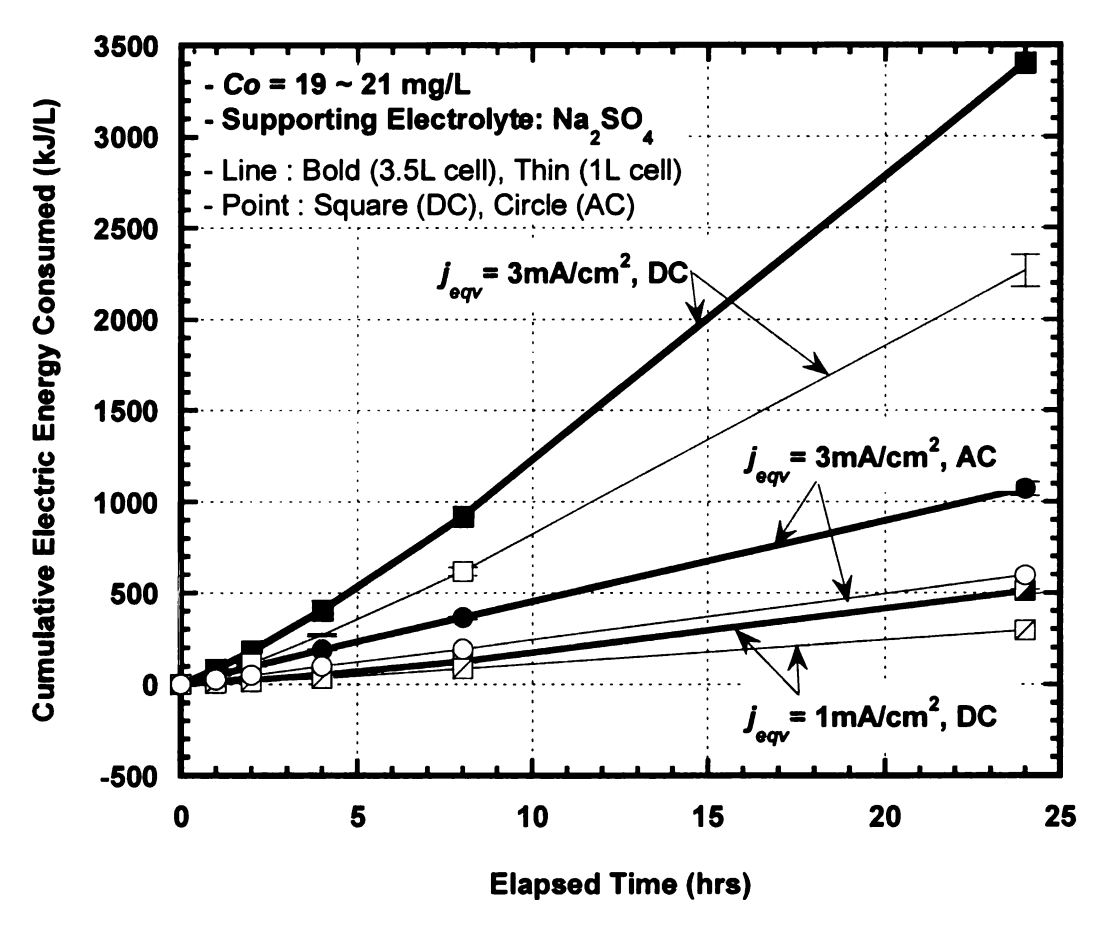


Figure 4.6: Normalized cumulative electrical energy consumed during electrochemical degradation of salicylic acid in aqueous phase experiments for j_{eqv} of 1 and 3 mA/cm² in 1 L and 3.5 L cells

4.1.3 Effect of Stirring During Electrochemical Degradation of Salicylic Acid

According to the *Nernst-Planck* equation (Eq. 2.11), mechanical stirring of electrolyte solution increases the mass flux of the target specie towards the electrodes. The increase in the flux will aid in increasing the rate of degradation (Pepprah 2007). It is due to convection. The effect of stirring was investigated because such data could be potentially used for sites where groundwater flow velocities can aid in transporting the chemical specie to the electrode(s) or where stirring can be used to decrease the current density to achieve an acceptable rate of degradation.

4.1.3.1 Degradation Kinetics

To evaluate the effect of stirring, the *pseudo*-first-order reaction (decay) equation was applied to the $\ln[C/C_0]$ versus time plots for all tests where the electrolyte was stirred or not stirred. The resulting degradation rate constants (k) and the resulting half-lives ($t_{1/2}$) for both cells are summarized in Table 4.6 and plotted in Fig. 4.7. For the 1 L cell, at j_{eqv} of 1 mA/cm² when DC was used, it yields k equal to 0.216 hr⁻¹ when the electrolyte was not stirred. When the electrolyte was stirred, k for the same cell increased to 0.458 hr⁻¹. It is more than two-fold increase. For the 3.5 L cell with DC, the increase in k was about three-fold and about four-fold for AC.

Table 4.6: Degradation rate constant (k) and the corresponding half-life $(t_{1/2})$ for salicylic acid tests in stirring aqueous solution (time period = 24 hours)

			1L cell			3.5L cell		
Current Type	<i>j _{eqv.}</i> (mA/cm²)	<i>k</i> (hr ⁻¹)	R²	<i>t _{1/2}</i> (hr)	<i>k</i> (hr ⁻¹)	R²	t _{1/2} (hr)	Remark
DC	3	0.216	0.998	3.2	0.167	0.996	4.1	.
	3	0.458	0.970	1.5	0.562	0.976	1.2	stirred
AC	3	0.033	0.989	20.9	0.031	0.990	22.4	
(f = 0.1 Hz)	3	-		-	0.137	0.978	5.0	stirred

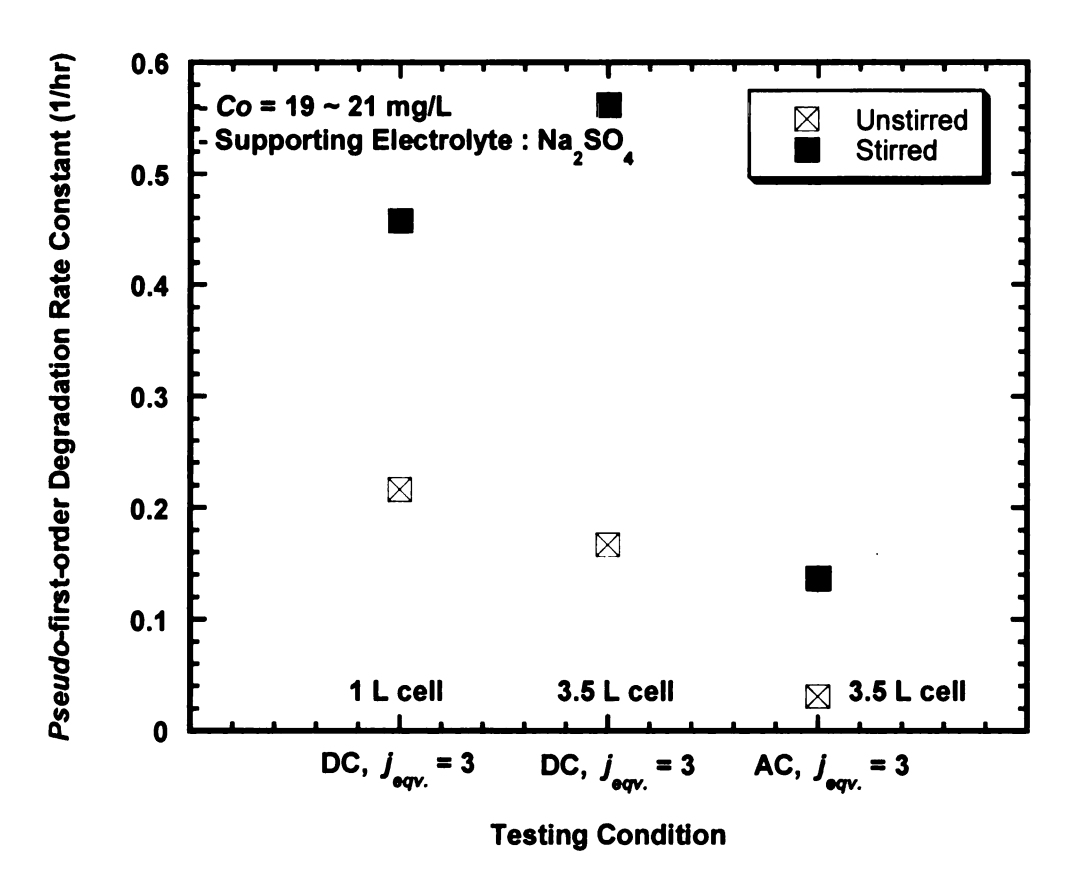


Figure 4.7: Variations of k observed for salicylic acid tests in aqueous solution with stirred or without stirred

4.1.3.2 Effect of Stirring on Degradation Rate of Salicylic Acid

Figure 4.8 shows the normalized concentration (C/C_o) of salicylic acid during tests when the electrolyte was continuously stirred using a magnetic stirrer. Both AC and DC applications were tested at j_{eqv} . Equal to 3 mA/cm². The ratio of C/C_o with stirring to C/C_o without stirring ranged from 3.2 for DC to 5 for AC at 8 hours of elapsed time. Pepprah and Khire (2008) have shown that Hydroxyl radicals (OH*) which are produced at the anode (or instantaneous anode for AC) are extremely potent oxidizing agents with a relatively short life, which is able to oxidize organic compounds by hydrogen abstraction reaction or by redox reaction as shown in Equation 4.3 and 4.4, respectively (Oturan 2000).

$$RH + OH^{\bullet} \rightarrow R^{\bullet} + H_2O \tag{4.3}$$

$$OH^{\bullet} + RX \rightarrow RX^{+\bullet} + OH^{-}$$
 (4.4)

In DC electrolysis, a cathode acts as a passive electrode, whereas in AC electrolysis, both electrodes participate in the reactions, switching their role as an anode and a cathode to each other. Hydroxyl radicals that act as a strong oxidant are produced in both electrodes when AC is used as a current mode and thus, stirring solutions contaminated with salicylic acid has a stronger effect in the mode of AC in the electrochemical degradation because both electrodes are able to react with the chemical more efficiently.

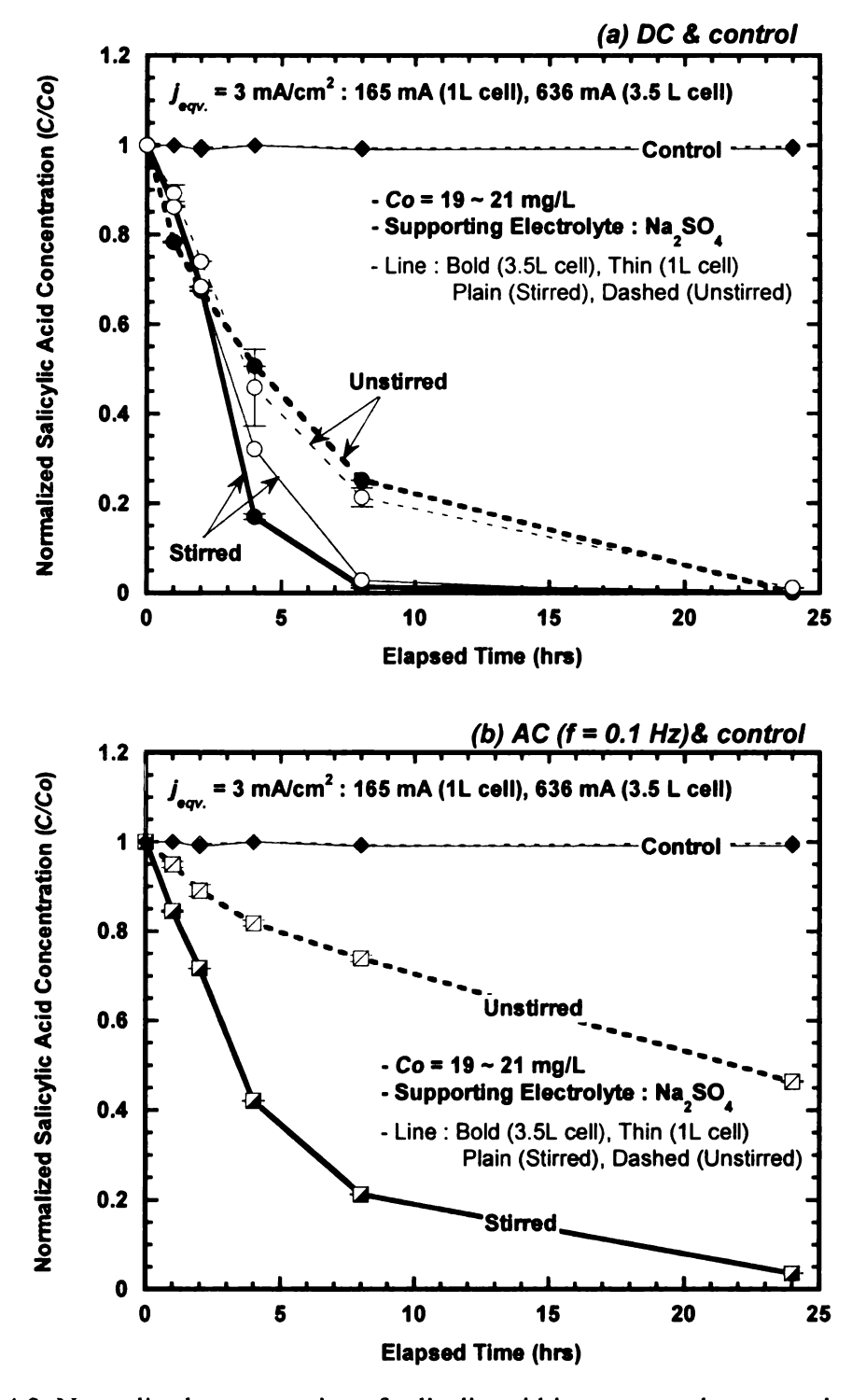


Figure 4.8: Normalized concentration of salicylic acid in aqueous phase experiments for DC (a) and AC (f = 0.1 Hz) (b) performed at $j_{eqv} = 3$ mA/cm² in 1 L and 3.5 L cells when stirred or unstirred

4.1.3.3 Cumulative Electrical Energy Consumption

4000 = 3 mA/cm²: 636mA (3.5L Cell) Cumulative Electrical Energy Consumed (kJ/L) 3500 $Co = 19 \sim 21 \text{ mg/L}$ DC, Stirred Supporting Electrolyte : Na SO 3000 2500 DC, Unstirred 2000 1500 AC (0.1Hz), Stirred 1000 500 AC (0.1Hz), Unstirred 5 10 15 20 25 Elapsed Time (hrs)

Line: Bold (3.5L cell), Thin (1L cell) / Plain (Stirred), Dashed (Unstirred) Point: Diamond (Control), Circle (DC), Square (AC)

Figure 4.9: Cumulative electrical energy consumed during electrochemical degradation of salicylic acid in aqueous phase experiments for DC and AC (f = 0.1 Hz) performed at $j_{eqv} = 3$ mA/cm² in 1 L and 3.5 L cells when stirred or unstirred

Figure 4.9 shows the cumulative electrical energy consumed during the electrochemical degradation of salicylic acid when the electrolyte was stirred or unstirred. Focusing on the electrical energy measured at the final elapsed time (24 hours), the gap between tests with a stirrer and without a stirrer is approximately 100 kJ per unit volume (one liter) regardless of AC or DC current modes. This difference is relatively small

4.1.3.4 Measured Initial and Final Test Parameters

Table 4.7 summarizes the measured initial and final values of key parameters - temperature, pH, standard redox potential, and electrical conductivity of the solution in the control and test cells.

Table 4.7: Summary of key parameters for salicylic acid tests in aqueous solution measured at initial and final time elapsed

.		Remarks			stirred		-			stirred
	ical :tivity m)			803			813	859	801	820
	Electrical Conductivity (µS/cm)	initial final (t=24hrs)		827			832	839	897	848
	Standard Redox Potential (mV)	final 24hrs)	537	304	351	472	356	797	375	868
	Standard Re Potential (mV)	initial (t=0hr)	558	358	467	449	377	370	396	380
	T	final (t=24hrs)	4.0	10.6	11.0	4.3	6.4	10.6	4.6	4.1
•	Ha	initial (t=0hr)	4.0	3.9	4.0	4.4	4.1	3.9	3.7	3.7
	Temperature (°C)	initial final (t=0hr) (t=24hrs)	19.6	25.2	25.7	18.1	24.1	33.3	23.1	24.1
`	ر) dweT	initial (t=0hr)	20.9	20.5	21.2	20.3	22.5	20.9	19.7	20.8
		Current (mA)	0	165	165	165	212	636	636	989
	Equivalent Current	Density (mA/cm ²)	0	3	3	3	1	3	3	3
-		Current Type	Control	20	oa	AC (0.1Hz)	DG	DC	3.5 L AC (0.1Hz)	3.5 L AC (0.1Hz)
		Cell	1	11	11	1 L	3.5 L	3.5 L	3.5 L	3.5 L

4.2 SANDY SOIL PHASE EXPERIMENTS

Table 4.8 outlines the summary of experimental variables used in Ottawa sand spiked with naphthalene or salicylic acid solution.

Table 4.8: Summary of experimental variables for sandy soil phase experiments

								Current	Density		
Compound	Medium	Cell Type	Supporting Electrolyte	Current Type	AC Frequency (Hz)	Equivalent Current Density (mA/cm ²)	Applied Current (mA)	Current Density (mA/cm ²)	(mA/L)	Stirring	Numbe of Tests
Naphthalene	Sand	1 L	Na ₂ SO ₄	Control			-				1
Naphthalene	Sand	1 L	Na ₂ SO ₄	AC	0.1	3	165	3	375		2
Naphthalene	Sand	1L	Na ₂ SO ₄	DC	0	3	165	3	375		1
Naphthalene	Sand	3.5 L	Na ₂ SO ₄	DC	0	1	212	1.19	125.37	The same	1
Salicylic Acid	Sand	1 L	Na ₂ SO ₄	DC	0	1.	55	1	125		2
Salicylic Acid	Sand	3.5 L	Na ₂ SO ₄	Control		Windows	7.00	A 12 mar		8	1
Salicylic Acid	Sand	3.5 L	Na ₂ SO ₄	AC	0.1	1	212	1.19	125.37		1
Salicylic Acid	Sand	3.5 L	Na ₂ SO ₄	DC	0	1	212	1.19	125.37	1	3
								Total nu	umber of	tests:	9

4.2.1 Naphthalene

4.2.1.1 Rate of Degradation

Figure 4.10 shows the normalized concentration (C/C_o) of naphthalene observed for experiments with 3.5 L cell with or without Ottawa sand, performed using DC application $(f_{eqv.} = 1 \text{ mA/cm}^2)$. The results from control experiments with and without sand (aqueous solution) are also presented in Fig. 4.10. For the tests with sandy media, samples were collected from the center of the cell as well as from points close to the anode and cathode to evaluate the spatial changes in concentration under the influence of applied current. For samples without sand, the concentration of naphthalene at the center of the cell was always less than when sand was present. For the sand sample, near anode,

due to oxidation occurring at the anode surface, the concentration of naphthalene was always less than that at the center or near the cathode. Thus, the presence of sandy soil slows down the rate of migration of naphthalene molecules to the anode where they are converted.

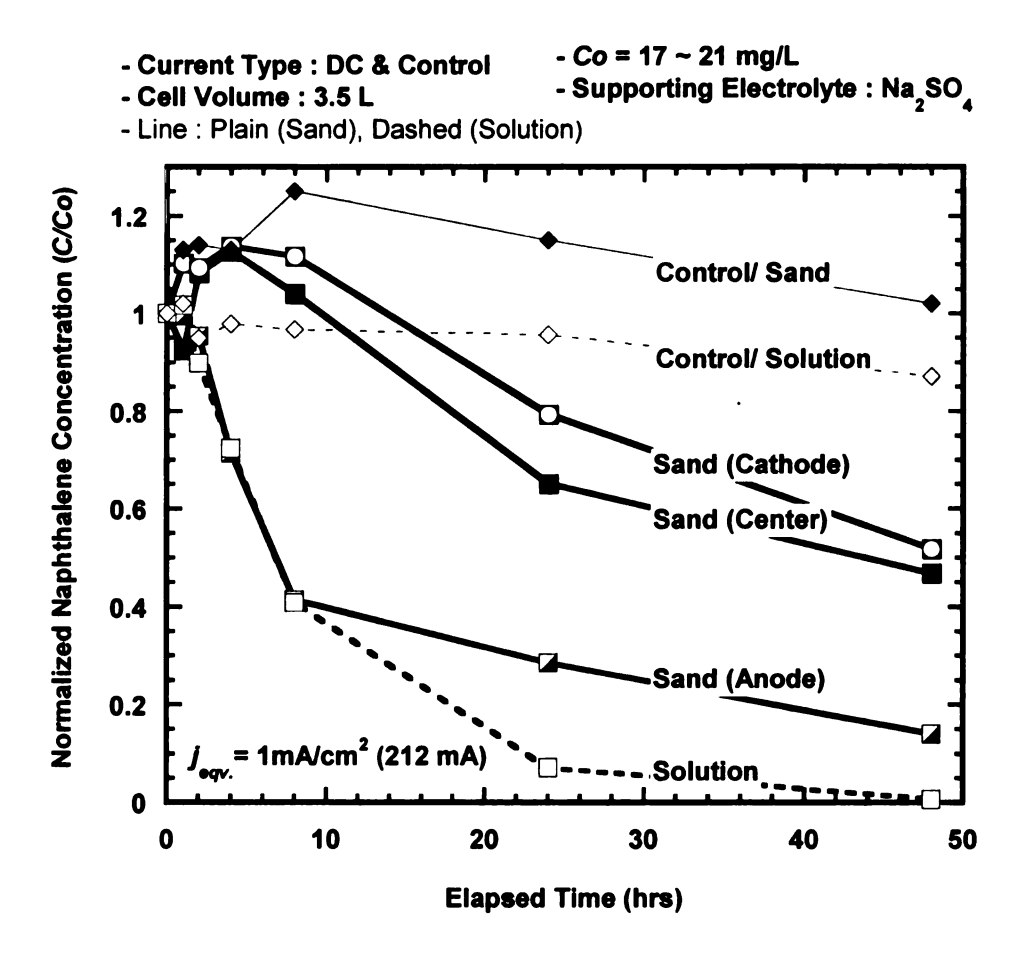


Figure 4.10: Normalized concentration of naphthalene for aqueous phase and sandy soil phase experiments for DC performed at $j_{eqv} = 1 \text{ mA/cm}^2$ (212 mA) for 3.5 L cell

4.2.1.2 Cumulative Electrical Energy Consumption

Compared with the aqueous phase experiment, the one with soil phase showed a nearly 50% increase in the cumulative electrical energy consumed during the 48 hour experiment as illustrated in Figure 4.11. The primary reason for increase in the electrical energy consumption in the presence of sand is increase in resistance due to the presence of sand displacing the electrolyte. Hence, for a given voltage, the experiments with sand required greater voltage. A greater amount of electrical energy was also used for Joule heating when sand was present.

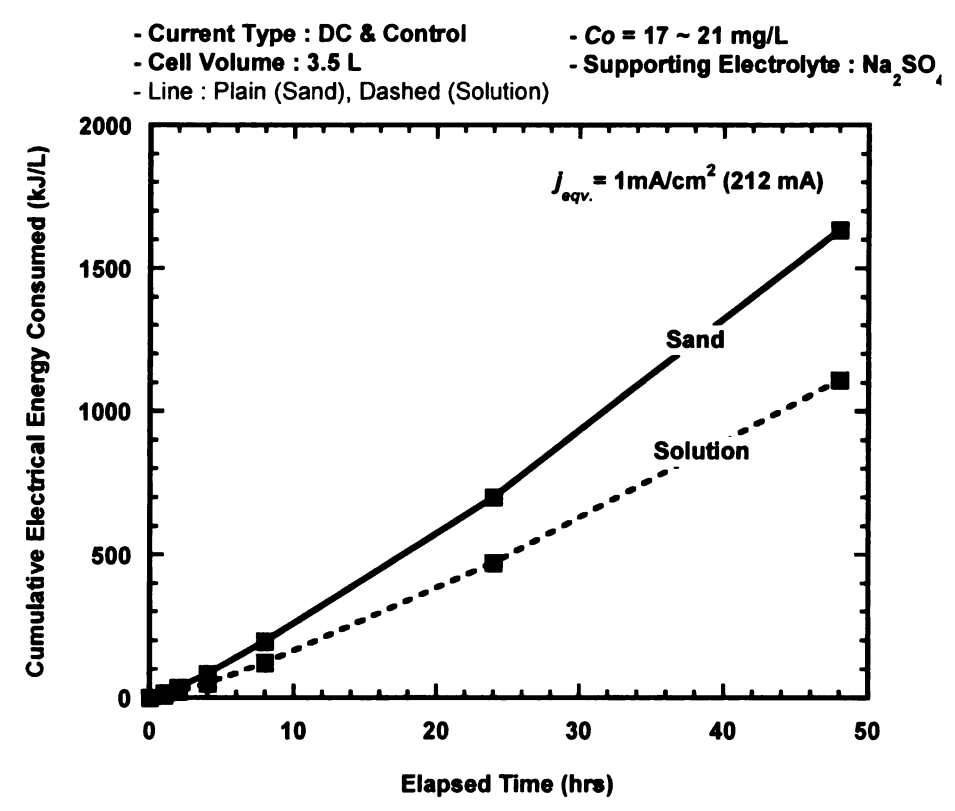


Figure 4.11: Cumulative normalized electrical energy consumed during degradation of naphthalene for aqueous phase and sandy soil phase experiments with DC performed at $j_{eqv} = 1 \text{ mA/cm}^2$ for 3.5 L cell

4.2.2 Salicylic Acid

As shown in Figure 4.12, about 40% and 60% degradation was recorded at the elapsed time of 8 hours in the 3.5 L cell when DC was applied for aqueous phase and soil phases, respectively. About, 65% and 80% degradation was observed in the 1 L cell. For both types of medium: aqueous solution and sandy soils, the control cell showed negligible loss of mass of salicylic acid.

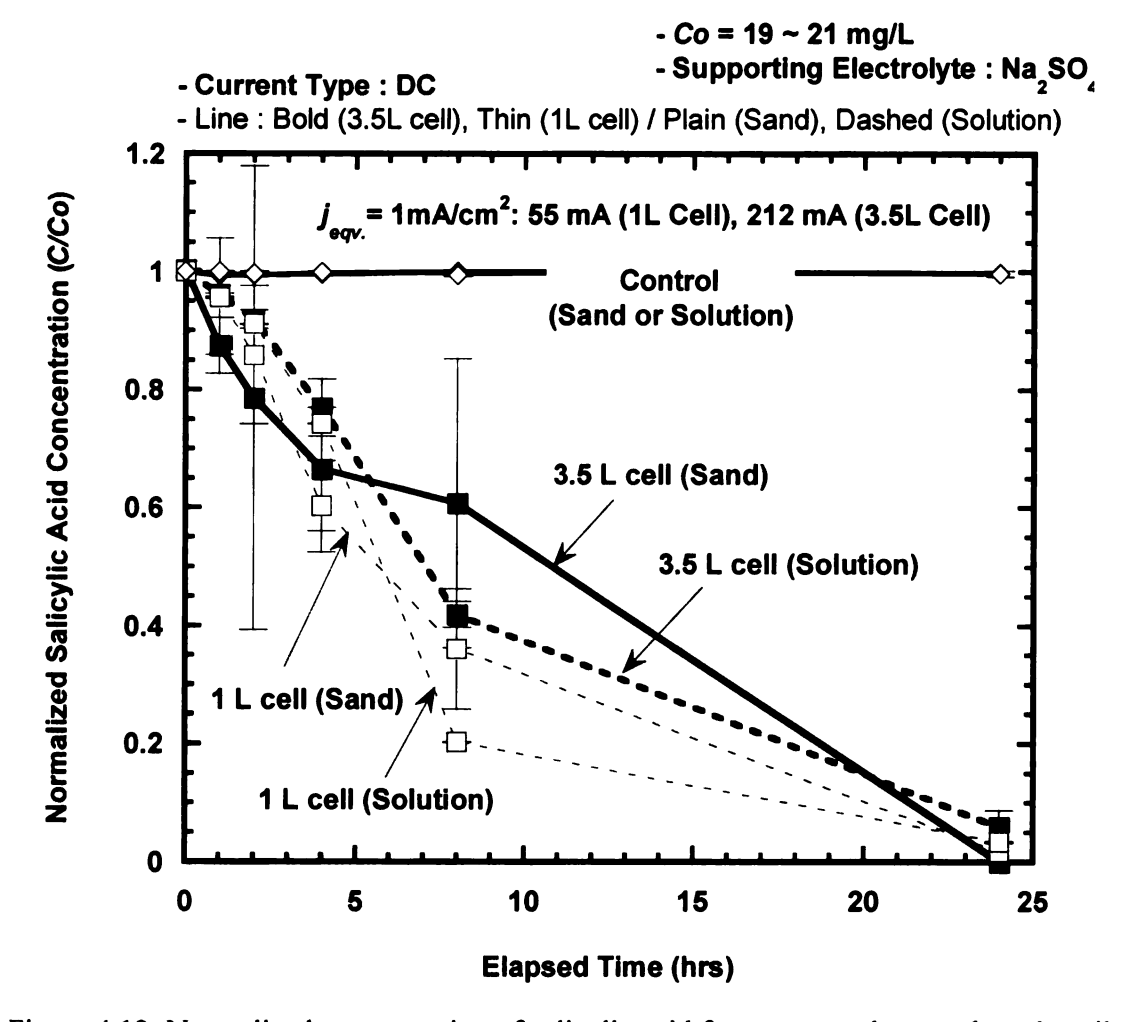


Figure 4.12: Normalized concentration of salicylic acid for aqueous phase and sandy soil phase experiments for DC performed at $j_{eqv} = 1 \text{ mA/cm}^2$ for 1 L and 3.5 L cells

The overall degradation of salicylic acid when sandy soil was present was slower than when only aqueous solution was tested.

Figure 4.13 shows the cumulative electrical energy consumed during the electrochemical degradation of salicylic acid in aqueous phase and sandy soil phase experiments. The figure shows the effect of not only the size of the cell but also of the media in the cell. The electrical energy consumed is lower when sandy phase is absent and the size of the cell increases the energy consumption.

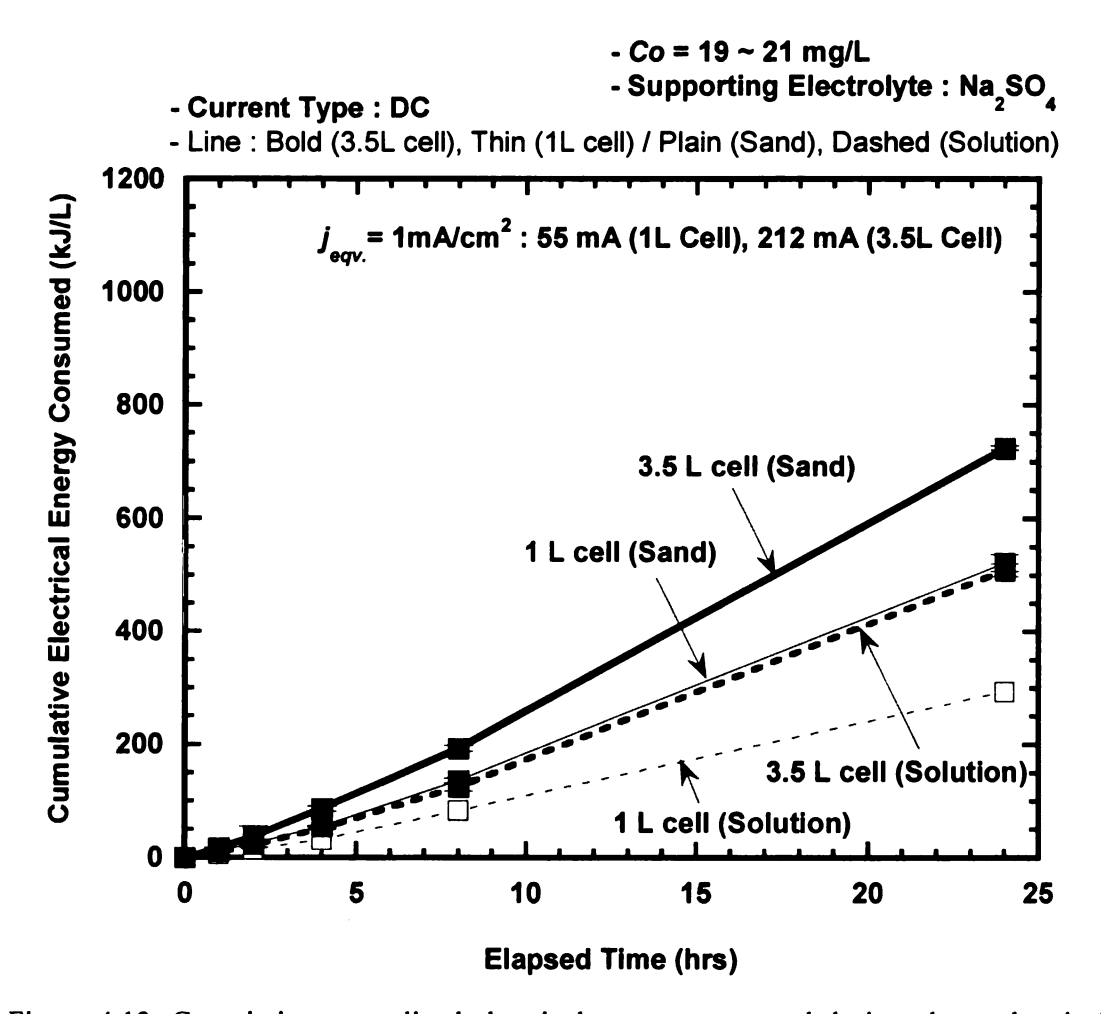


Figure 4.13: Cumulative normalized electrical energy consumed during electrochemical degradation of salicylic acid in aqueous phase and sandy soil phase experiments for DC performed at j_{eqv} , of 1 mA/cm² in 1 L and 3.5 L cells

Similar to the naphthalene tests in Ottawa sand, samples were collected at these three points: in the vicinity of the anode and cathode, and at the center point between the electrodes. The results are presented in Fig. 4.14 in the form of normalized concentrations (C/C_o) of salicylic acid versus elapsed time for DC and AC applications. Fig. 4.14(a) shows these results for the DC tests where the normalized concentrations were least at the cathode and progressively increased towards the center and cathode. At cathode, the normalized concentration of salicylic acid reached about 4 as the experiment progressed. The normalized concentration was always less than one when AC was used with salicylic acid (Fig. 4.14b) or when naphthalene was tested with DC (Fig. 4.10).

The concentration gain at the cathode can be explained by adsorption of salicylic acid on the sand particles in the vicinity of the cathode (-ve electrode). Xu et al. (2007) investigated the adsorption of salicylic acid on two variable charge soils (a Rhodic Ferralsol and a Haplic Acrisol). At an initial concentration of 1.0 mM, the adsorption of salicylic acid by the Haplic Acrisol and Rhodic Ferralsol was 9.2 and 13.3 mmol kg⁻¹, respectively. Iron and aluminum oxides in variable charge soils are key adsorbents for anions, and the greater the content of the oxides in a soil, the larger the amount of the organic acid adsorbed. The presence of oxidants in the solution mixed with DI water and Ottawa sand was analyzed for Ca²⁺. Ca²⁺ concentration was about 1.39 mg/L. Thus, the sand around cathode provided sites where the organic acid was adsorbed during the DC application. Fig. 4.14 (a) shows that the amount of the adsorption at the cathode in the 3.5 L cell is larger than in the 1 L cell. It supports that the soil particles surrounding a larger surface area of the electrode (the 3.5 L cell) provide more adsorption sites for salicylic acid than those on a smaller surface area.

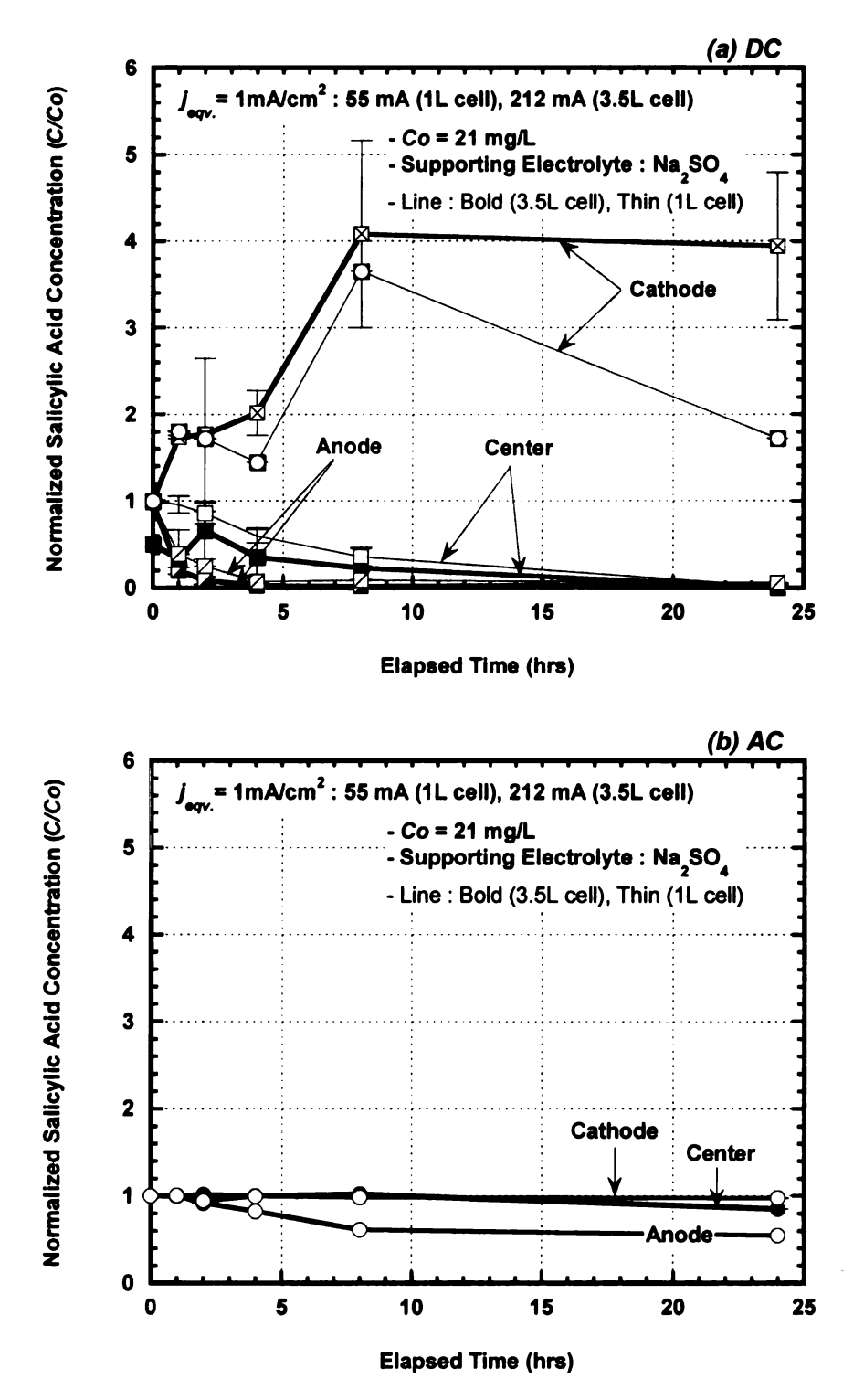


Figure 4.14:Normalized concentration of salicylic acid in sandy soil phase experiments for DC (a) and AC (f = 0.1 Hz) (b) performed at $j_{eqv} = 1$ mA/cm² in 1 L and 3.5 L cells

The adsorption explanation used for DC (Fig. 4.15) can be further strengthened when concentration data for AC (f = 0.1 Hz) application shown in Fig. 4.14(b) is studied. Because the anode and cathodes are being swapped in every AC cycle, the concentration gain due to adsorption observed at the cathode in the DC test was not present at both electrodes during the AC test. All concentration ratios were one or below. Therefore, in summary, presence of Ca^{2+} as an oxidant and the temporary cation exchange capacity created by the negatively charged electrode (cathode) in the sand can be attributed for the adsorption of the organic acid on the cathode resulting in an increase in concentration of salicylic acid at the cathode during DC test.

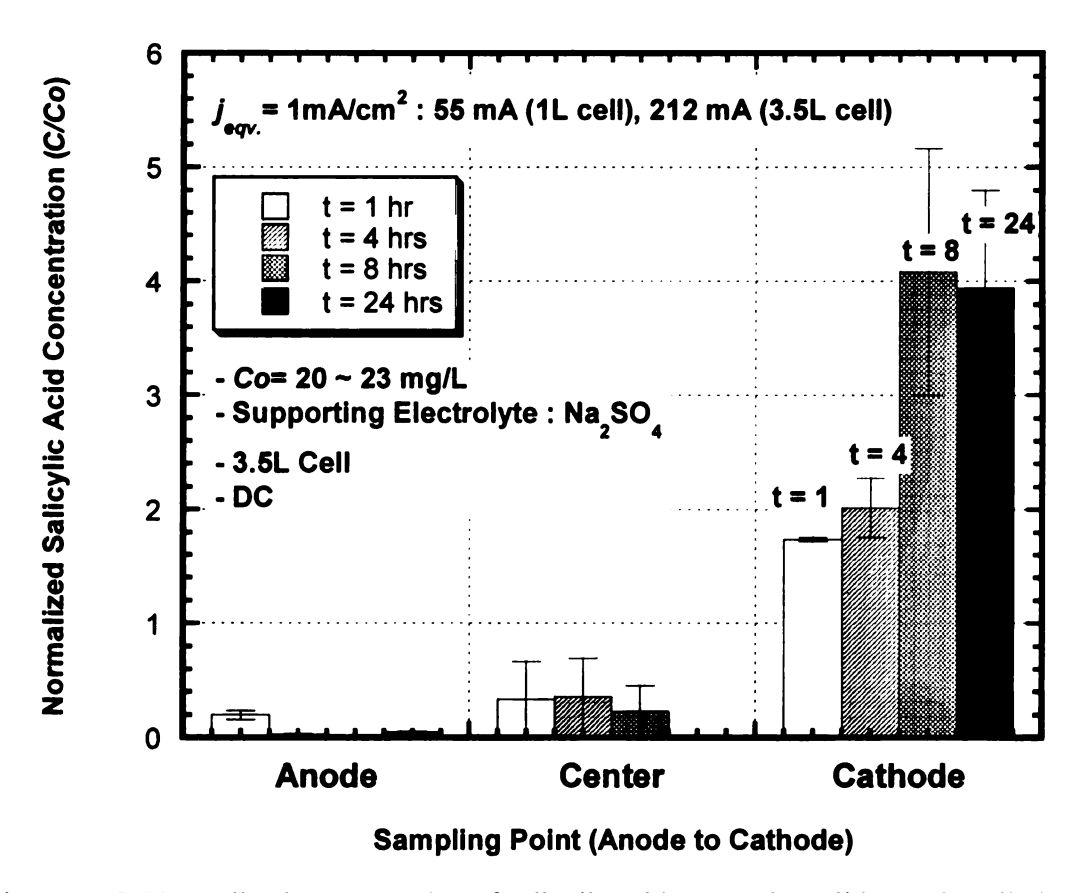


Figure 4.15: Normalized concentration of salicylic acid across the cell in sandy soil phase experiments for DC performed at $j_{eqv} = 1 \text{ mA/cm}^2$ (212 mA) for 3.5 L cell

Apart from monitoring the aqueous phase concentrations of salicylic acid over time, other experimental parameters including temperature, pH, standard redox potential, electrical conductivity were measured at initial (t = 0 h) and final (t = 24 h) elapsed times. Table 4.10 presents the results.

Table 4.10: Summary of key parameters for salicylic acid tests in sandy soil measured at initial and final time elapsed

			Equivalent Current		Jemp ()	Temperature (°C)	<u>α</u> .	H	Standar Pote (m	Standard Redox Potential (mV)	Elec Cond	Electrical Conductivity (μS/cm)	Medium
Supporting Current Density Cu	Density	Density Cu	ರ	Irrent	Current initial	final	initial	final	initial	initial final	initial	final	
Electrolyte Type (mA/cm²) (mA)	(mA/cm²)	- 1	- 1	a	(t=0hr)	(t=0hr) (t=24hrs) (t=0hr) (t=24hrs) (t=0hr) (t=24hrs) (t=0hr) (t=24hrs)	(t=0hr)	(t=24hrs)	(t=0hr)	(t=24hrs)	(t=0hr)	(t=24hrs)	
Na ₂ SO ₄ Control 0 0	Control 0 0	0 0	0		20	44.1	7.20	8.00	420	394	867	1052	Sand
Na ₂ SO ₄ Control 0 0	Control 0 0	0 0	0		19.9	19.6	6.70	6.70	458	469	811	815	Solution
Na ₂ SO ₄ AC (0.1Hz) 3 165	3	3 165	165		20.1	20.8	6.80	11.50	339	184	835	1297	Sand
Na ₂ SO ₄ AC (0.1Hz) 3 165	3	3 165	165		19.2	18	6.50	4.50	394	415	811	818	Solution

4.3 ANALYTICAL MODELING USING NERNST-PLANCK EQUATION

It is well understood that electrochemical reactions primarily occur on the surface or in the vicinity of electrodes and thus, the rate of degradation would be predictable if reactions taking place on the surface of the electrodes are defined and modeled. The reactions are represented by direct/indirect oxidation processes and can be related to the mass transfer to the electrode expressed in the *Nernst-Planck Equation* (Eq. 2.11). Eq. 2.11 shows the three terms corresponding to the three modes of mass transfer to the electrodes: diffusion, migration, and convection. If the test cell is not stirred, the third term (convection) in Equation 2.11 is disregarded and the equation becomes (Eq. 4.5):

$$J_{i}(x) = -D_{i}(x)\frac{\partial C_{i}(x)}{\partial x} - \frac{z_{i}F}{RT}D_{i}C_{i}\frac{\partial \phi(x)}{\partial x}$$
(4.5)

Again, for the uncharged reactant, the second term (migration) in Equation 2.11 can be neglected and then the equation becomes (Eq. 4.6):

$$J_{i}(x) = -D_{i}(x)\frac{\partial C_{i}(x)}{\partial x}$$
(4.6)

In this section, the mass flux obtained by the two terms - diffusion and migration - and the resulting concentration of a pollutant are predicted using Equation 4.5 and 4.6 based on the *Nernst-Planck* equation. This approach was not applied to the stirred experiments because the convection velocities were not measured during the tests.

4.3.1 Key Assumptions

The assumptions followed when applying Eq. 4.5 are presented as follows.

- Reactants (naphthalene and salicylic acid) are instantaneously converted (degraded) to products when they come into contact with the electrode (in this case anode). Hence, concentration versus time (t) at the surface of electrode is equal to zero at $t \ge 0$ hr. This establishes a concentration gradient that drives reactants by diffusion to the surface of the electrodes and this condition is considered as the maximum concentration gradient that may be established in a given time step;
- Steady-state diffusion is assumed during the time step of 1 hr; and
- Linear mass transfer and electric field exist in the cell between the electrodes.

4.3.2 Naphthalene

The diffusion coefficient (*D*) was estimated before applying Eq. 4.5 as it is one of the required input parameters. As introduced in Equation 2.12, the Hayduk-Laudie's relationship (1974) was used to estimate the diffusion coefficient (*D*) of naphthalene. After interpolating the solution viscosity at a given temperature, using the molar volume of naphthalene ($\sim 125.7 \text{ cm}^3 \text{ mol}^{-1}$), and plugging these parameters into Equation 2.12, *D* for naphthalene at various temperature conditions ranged from 1.0×10^{-5} to 4.0×10^{-6} cm² s⁻¹. Schwarzenbach *et al.* (2003) have reported diffusion coefficients of organic solutes equal to about $3.0 \times 10^{-5} \text{ cm}^2 \text{ s}^{-1}$ for relatively small molecules to $5.0 \times 10^{-6} \text{ cm}^2 \text{ s}^{-1}$ for those of molar mass near 300 g mol⁻¹.

The observed and simulated normalized concentrations when both diffusion and migration are used for simulating the mass flux of naphthalene to the anode are presented in Figure 4.16.

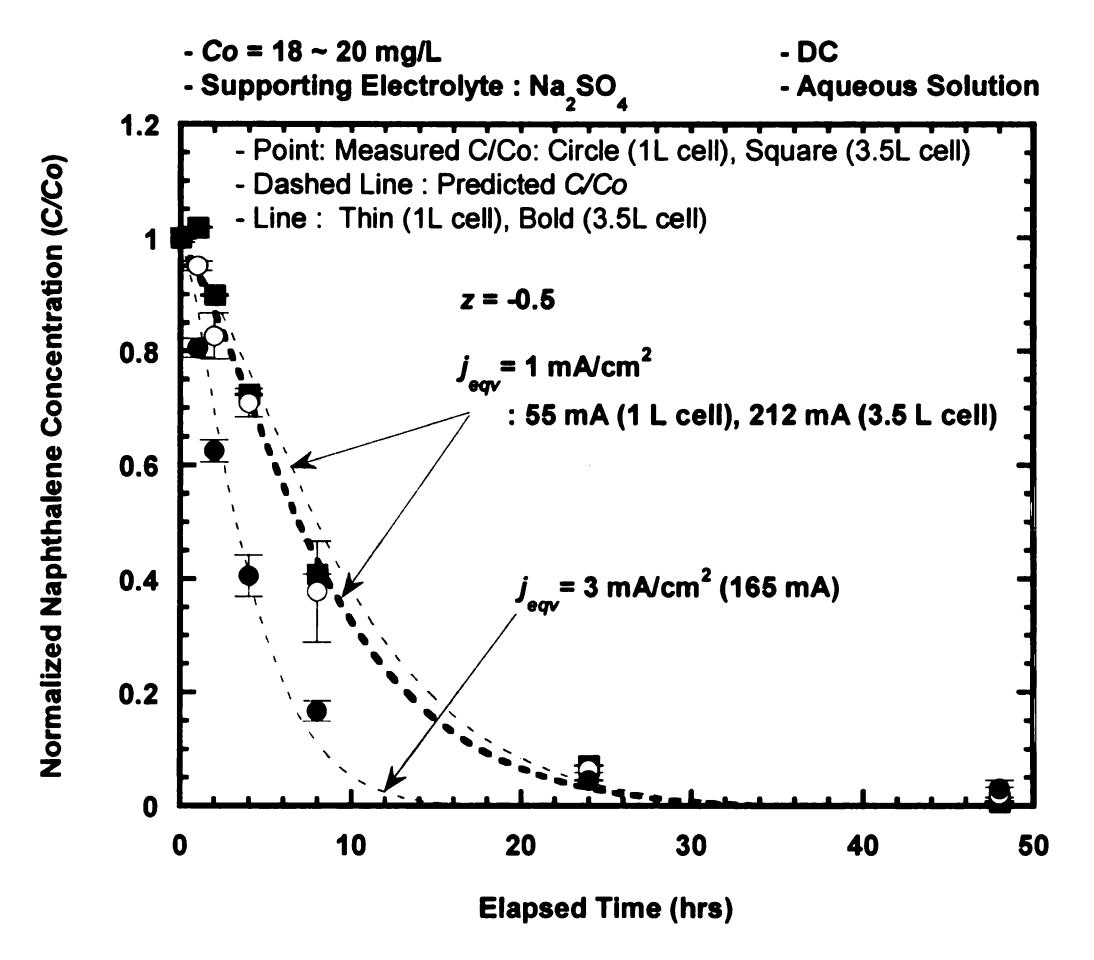


Figure 4.16: Experimental and predicted concentration rations of naphthalene for $j_{eqv} = 1$ and 3 mA/cm² in 1 L and 3.5 L cells for DC application

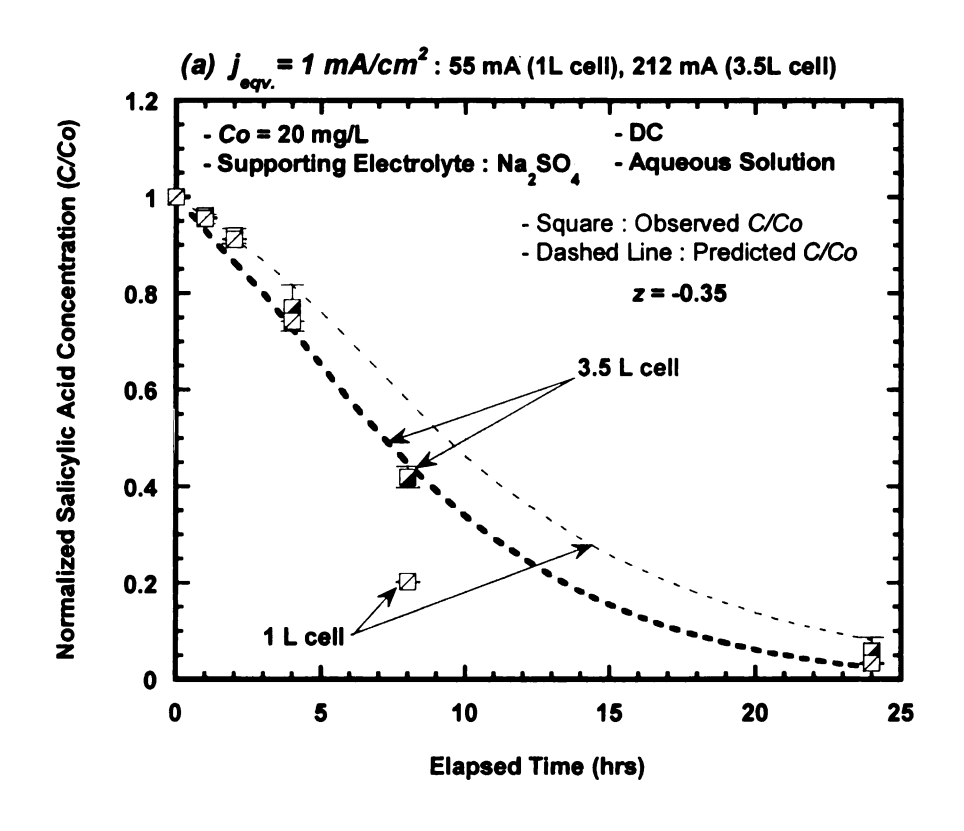
For the simulations using Equation 4.5, the value of net charge (z) was empirically obtained from the best fit to the measured concentration profile. The best fit was obtained when z was assumed equal to -0.50. Pepprah (2007) also obtained the same z for experiments carried on 1 L cells. While the z value should be zero for naphthalene because the naphthalene molecule is neutral. However, it is hypothesized that the anions in the supporting electrolyte (anhydrous sodium sulfate) drag naphthalene to the anode. Fig. 4.16 shows a relatively accurate prediction of concentration changes for the 1 L and 3.5 L cells.

4.3.3 Salicylic Acid

As discussed in section 4.1.2.4, the rate of salicylic acid degradation in the 1 L cell was recorded slightly higher than the one in the 3.5 L cell. To further this finding, it is necessary to simulate the degradation rates and compare between the observed and predicted concentrations using Equation 4.5 where the key parameters: temperature and voltage measured in tests were used. For simulations, the net charge (z) and the diffusion coefficient (D) for salicylic acid were obtained from Pepprah (2007). The value of z was assumed equal to -0.35 and D ranged from 1.17×10^{-5} to 4.65×10^{-6} cm² s⁻¹ as a function of measured temperature.

Figure 4.17 shows the experimental and predicted concentration ratios of salicylic acid for j_{eqv} . Equal to 1 and 3 mA/cm² for both cells. Overall the predicted concentration rations are close to the measured values. However, for the 1 L cell, the predicted values are underestimated. Whereas those values for the 3.5 L cell are slightly overestimated. The predicted curves show faster degradation in the 3.5 L which is opposite to what is observed from the experiments.

The *Nernst-Planck* equation does not include the effect of size or surface area of the electrodes. A majority of the reactions (degradation) occur at the surface of the electrode. The ratio of the surface area of electrodes over the volume of the cell is 55 cm²/L and 50.9 cm²/L for the 1 L and the 3.5 L cells, respectively. The ratio is slightly lower for the 3.5 L cell. This may be the reason why the observed rate of degradation in the 3.5 L cell was less than the 1 L cell. However, the *Nernst-Planck* equation does not simulate the effect of electrode area.



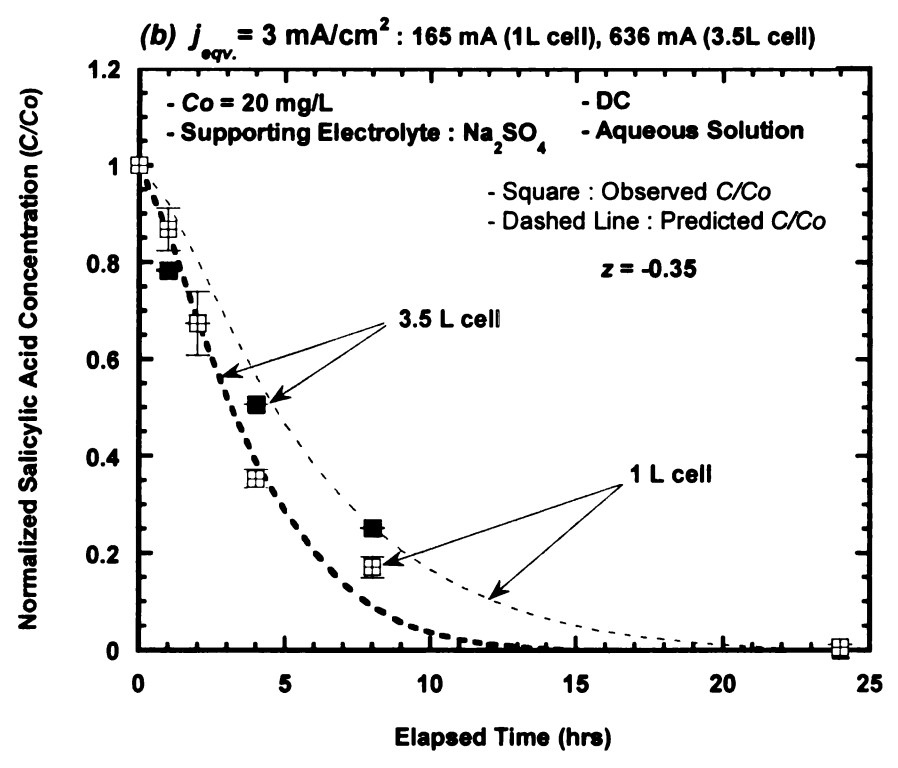


Figure 4.17: Experimental and predicted concentration ratios of salicylic acid for $j_{eqv} = 1$ mA/cm² (a) and 3 mA/cm² (b) in 1 L and 3.5 L cells

CHAPTER 5

SUMMARY AND CONCLUSIONS

The key objectives of this study were to evaluate the effect of scale during electrochemical degradation of naphthalene and salicylic acid in aqueous as well as sandy soils phases. The effect of scale was evaluated by measuring the rate of degradation and electrical energy consumption for experiments carried out at using AC and DC at two current densities for cells having 1 L and 3.5 L volume.

- Degradation rates increased as the current density was increased for both 1 L and
 3.5 L cells.
- 2. For an equivalent current density expressed in the form of current per unit volume of the electrolyte. The rate of degradation was virtually independent of the scale of the cell. However, the electrical energy consumption was two to four folds more for the larger cell. Thus, larger cell was not as energy efficient as the smaller cell. Greater resistance of the larger cell resulting in greater joule heating and loss of energy may be the reason for greater energy consumption.
- Degradation kinetics observed in the aqueous phase experiments could be fitted
 by the *pseudo*-first order decay model when naphthalene and salicylic acid were
 used as contaminants.
- 4. In the presence of sandy soil phase, adsorption of organic acid on the sand particles near cathode yielded greater than one concentration ratios. This was attributed to the presence of Ca⁺⁺ and oxides in the sand and negatively charged cathode creating temporary cation exchange capacity for the sand particles.

- 5. Stirring significantly enhanced the rate of degradation for both AC and DC. However, it was more significant for AC. Stirring accelerates the electromigration of the species to the electrodes (anode for the chemicals studied) where it can be converted.
- 6. Nernst-Planck equation simulating migration of the chemical specie to the electrodes using electromigration and diffusion simulated concentration rations that agreed relatively well with the measured values. Thus, both diffusion and electromigration processes contributed to the rate of mass transfer of naphthalene as well as salicylic acid to the reaction sites (e.g. on the surface of electrodes or in the vicinity of electrodes) without convection unless the solution was stirred. However, migration was the dominant mass transfer process when stirring was not carried out.

REFERENCES

- Acar, Y. B., and Alshawabkeh, A. N., "Electrokinetic remediation. I. Pilot-scale tests with lead-spiked kaolinite", J. Geotech. Eng., 122(3), 173-185 (1996).
- Agency for Toxic Substances and Disease Registry (ATSDR), "Toxicological profile for naphthalene (updated)", Atlanta, GA: U.S. Department of Health and Human Services, Public Health Service (1995).
- Agency for Toxic Substances and Disease Registry (ATSDR), "ToxFAQs™ for naphthalene, 1-methylnapthalene, 2-methyl naphthalene",
- http://www.atsdr.cdc.gov/toxfaq.html. Atlanta, GA: U.S. Department of Health and Human Services, Public Health Service (2005).
- Alshawabkeh A. N., and Sarahney, H., "Effect of current density on enhanced transformation of naphthalene", *Environ. Sci. Tech.*, 39, 5837-5843 (2005).
- Alshwabkeh, A. N., and Acar, Y. B., "Electrokinetic remediation. II. Theoretical model", J. Geotech. Eng., 122(3), 186-196 (1996).
- Bamforth, S. M. and Singleton, I., "Review: Bioremediation of polycyclic aromatic hydrocarbons: Current knowledge and future directions", *J. Chem. Tech. Biotech.*, **80**(7), 723-736 (2005).
- Bard, A. J., and Faulkner, L. R., "Electrochemical methods: fundamentals and applications", John Wiley & Sons Inc., New York (2001).
- Canizares, P., Lobato, J., Garcia-Gomez, J., and Rodrigo, M. A., "Combined adsorption and electrochemical process for the treatment of acidic aqueous phenol wastes", J. Appl. Electrochem., 34, 111-117 (2004).
- Canizares, P., Lobato, J., Paz, R., Rodrigo, M. A., and Saez, C., "Electrochemical oxidation of phenolic wastes with boron-doped diamond anodes", *Water Res.*, 39, 2687-2703 (2005).
- Carvalho, C., Fernandes, A., Lopes, A., Pinheiro, H., and Goncalves, I., "Electrochemical degradation applied to the metabolites of acid orange 7 anaerobic biotreatment", *Chemosphere*, 67, 1316-1324 (2007).
- Chen, G. H., "Electrochemical technologies in wastewater treatment", Sep. Purif. Tech., 38, 11-41 (2004).

- Chen. W. P., Wang, Y., Wang, X. X., Wang, J., and Chan, H. L. W., "Water-induced DC and AC degradation in TiO2-based ceramic capacitors", *Materials Chemistry and Physics*, 82(3), 520-524 (2003).
- Chiang, L. C., Chang, J. E., and Wen, T. C., "Indirect oxidation effect in electrochemical oxidation treatment of landfill leachate", *Water Res.*, 29(2), 671-678 (1995).
- Chin, D. T., and Cheng, C. Y., "Oxidation of phenol with AC Electrolysis", J. Electrochem. Soc., 132 (11), 2605-2611 (1985).
- Clar, E., "Polycyclic hydrocarbons", Academic Press, New York (1964).
- Comninellis, Ch., and Pulgarin, C., "Anodic oxidation of phenol for waste water treatment", J. Appl. Electrochem., 21, 703-708 (1991).
- Crittenden, J. C., Trussell, R. R., Hand, D. W., Howe, K. J., and Tchobanoglous, G., "Water treatment: principle and design", John Wiley & Sons Inc., New Jersey (2005).
- Feng, Y. J., and Li, X. Y., "Electro-catalytic oxidation of phenol on several metal-oxide electrodes in aqueous solution", *Water Res.*, 37, 2399-2407 (2003).
- Goel, R. K., Flora, J. R. V., and Ferry, J., "Mechanisms of naphthalene removal during electrolytic aeration", Water Res., 37, 891-901 (2003).
- Grimm, J., Bessarabov, D., and Sanderson, R., "Review of electro-assisted methods for water purification", *Desalination*, 115, 285-294 (1998).
- Harvey, R. G., "Polycyclic Aromatic Hydrocarbons", Wiley-VCH, Inc., New York (1997).
- Hayduk, W., and H. Laudie, "Prediction of diffusion coefficient for non-electrolytes in dilute aqueous solutions", AlChE J., 20, 611-615 (1974).
- Centers for Disease Control (CDC), "International Chemical Safety Cards (ICSC): Naphthalene", http://www.cdc.gov/niosh/ipcsneng/neng0667.html (2005).
- Centers for Disease Control (CDC), "International Chemical Safety Cards (ICSC): Salicylic acid", http://www.cdc.gov/niosh/ipcsneng/neng0563.html (1997).
- Iniesta, J., Gonzalez-Garcia, J., Expósito, E., Montiel, V., and Aldaz, A., "Influence of chloride ion on the electrochemical degradation of phenol in alkaline medium using bismuth doped and pure PbO2 anodes", *Water Res.*, **35**, 3291-3300 (2001).
- Iniesta, J., Michaud, P. A., Panizza, M., Cerisola, G., Aldaz, A., and Comninellis, Ch., "Application of synthetic boron-doped diamond electrode in electro-oxidation and in electro-analysis", *Electrochim. Acta*, 46, 3573-3578 (2001).

- Li X. Y., Cui, Y. H., Feng, Y. J., Xie, Z. M., and Gu, J. D., "Reaction pathways and mechanisms of electrochemical degradation of phenol on different electrodes", *Water Res.*, 39, 1972-1981 (2005).
- Li, Y., Wang, F., Zhou, G., and Ni, Y., "Aniline degradation by electrolytic oxidation", *Chemosphere*, **53**(10), 1229-1234 (2003).
- Louhichi, B., Bensalash, N., and Gadri, A., "Electrochemical oxidation of benzoic acid derivatives on boron doped diamond: Volta metric study and galvanostatic electrolyses", *Chem. Eng. Tech.*, **29**(8), 944-950 (2006).
- Montilla, F., Michaud., P. A., Morllon, E., Vazquez., J. L., and Comninellis, Ch., "Electrochemical oxidation of benzoic acid at boron-doped diamond electrodes", *Electrochim. Acta*, 47, 3509-3513 (2002).
- Nakamura, A., Hirano, K., and Iji, M., "Decomposition of trichlorobenzene with different radicals generated by alternating current electrolysis in aqueous solution", *Chemistry Letters*, **34**(6), 802-803 (2005).
- Oturan, M. A., "An ecologically effective water treatment technique using electrochemically generated hydroxyl radicals for *in situ* destruction of organic pollutants: Application to herbicide 2,4-D", *J. Appl. Electrochem.*, 30(4), 475-482 (2000).
- Panizza, M., Bocca, C., and Cerisola, G., "Research note: Electrochemical treatment of wastewater containing polyaromatic organic pollutants", *Water Res.*, **34**, 2601-2605 (2000).
- Panizza, M., Kapalka., A. K., and Comninellis, Ch., "Oxidation of organic pollutants on BDD anodes using modulated current electrolysis", *Electrochim. Acta*, **53**, 2289-2295 (2008).
- Pepprah, E., "Degradation of Polycyclic Aromatic Hydrocarbons (PAHs) in Aqueous Media using Alternating Current." Ph.D. Dissertation, Michigan State University (2007).
- Pepprah, E., and Khire, M. V., "Electroremediation of naphthalene in aqueous solution using alternating and direct currents", J. Environ. Eng., 134(1), 32-41 (2008).
- Qiang, Z., Chang, J. H., and Huang, C. P., "Electrochemical generation of hydrogen peroxide from dissolved oxygen in acidic solutions", *Water Res.*, 36, 85-94 (2002).
- Rajeshwar, K., Ibanez, J. G., and Swain, G. M., "Electrochemistry and the environment", J. Appl. Electrochem., 24(11), 1007 (1994).

- Rodgers, J. D., Jedral, W. J., N.J. and Bunce, N. J., "Electrochemical oxidation of chlorinated phenols", *Environ. Sci. Tech.*, 33, 1453-1457 (1999).
- Saracco G., Solarino, L., Aigotti, R., Specchia, V., and Maja, M., "Electrochemical oxidation of organic pollutants at low electrolyte concentrations", *Electrochim. Acta*, 46, 373-380 (2000).
- Sarahney, H., and Alshawabkeh, A. N., "Effect of current density on electrolytic transformation of benzene for groundwater remediation", *J. Haz. Materials*, **143**, 649-654 (2007).
- Schwarzenbach, R. P., Gschwend, P. M., and Imboden, D. M., "Environmental Organic Chemistry", John Wiley & Sons, Inc., New Jersey (2003).
- Simond, O., Schaller V., and Comninellis, Ch., "Theoretical model for the anodic oxidation of organics on metal electrodes", *Electrochim. Acta*, 42, 2009-2012 (1997).
- Stock N. L., and Bunce, N. J., "Electrocatalytic dechlorination of atrazine", Can. J. Chem., 80, 2000-2006 (2002).
- Tahar, N. B., and Savall, A., "Mechanistic aspects of phenol electrochemical degradation by oxidation on a Ta/PbO2 Anode", J. Electrochem. Soc., 145(10), 3427-3573 (1998).
- Titanium Information Group, *Titanium and the Environment*, Data Sheet, 19(1) (2002, April 1).
- US EPA, "Permeable reactive barrier technologies for contaminant remediation", EPA/600/R-98/125(1998).
- US EPA, "A citizen's guide to bioremediation", EPA 542-F-01-001 (2001a).
- US EPA, "A citizen's guide to permeable reactive barriers", EPA 542-F-01-005 (2001b).
- US EPA, "Health effect support document for naphthalene", http://www.epa.gov/safewater/ccl/pdf/naphthalene.pdf (2003).
- US EPA, "Technical Factsheet on: Polycyclic Aromatic Hydrocarbons (PAHs)", http://www.epa.gov/safewater/dwh/t-soc/pahs.html (2006).
- US EPA, "Treatment of technologies for mercury in soil, waste, and water", WA: Office of superfund remediation and technologies (2007).
- Wu, D., Liu, M., Dong, D., and Zhou, X. "Effects of some factors during electrochemical degradation of phenol by hydroxyl radicals", *Microchem. J.*, **85**, 250-256 (2007).

Xu, R. K., Xiao, S. C., Zhang, H., Jiang, J., Ji, G. L., "Adsorption of phthalic acid and salicylic acid by two variable charge soils as influenced by sulphate and phosphate" *European J. Soil Sci.*, **58**, 335-342 (2007).

